



RESEARCH PAPER

## A mathematical model to investigate the effect of misdiagnosis and wrong treatment in the co-circulation and co-infection of Malaria and Zika virus disease

Emmanuel C. Duru <sup>1,\*,\ddagger</sup>, Michael C. Anyanwu <sup>1,\ddagger</sup> and Godwin C.E. Mbah <sup>2,\ddagger</sup>

<sup>1</sup>Department of Mathematics, Michael Okpara University of Agriculture, P.M.B. 7267 Umudike, Abia State, Nigeria, <sup>2</sup>Department of Mathematics, University of Nigeria, P.M.B. 3147 Nsukka, Enugu State, Nigeria

\* Corresponding Author

\ddagger duru.emmanuel@mouau.edu.ng (Emmanuel C. Duru); manyanuw71@yahoo.com (Michael C. Anyanwu); godwin.mbah@unn.edu.ng (Godwin C.E. Mbah)

### Abstract

Malaria and Zika virus disease are infectious diseases transmitted among humans through the bites of an infectious female Anopheles and Aedes aegypti mosquitoes, respectively. In areas where the two diseases co-circulate, their coinfection is possible. Both diseases exhibit similar characteristic symptoms, hence one can be misdiagnosed as the other. In this work, we use a system of nonlinear ordinary differential equations to present a new model for the coinfection of the two diseases. The dynamics of the individual diseases are also shown. The disease-free equilibrium (DFE) points of the individual diseases are seen to be both locally and globally asymptotically stable when their respective basic reproduction numbers are less than one. But, the coinfection-free equilibrium (CFE) is seen to be only locally asymptotically stable when the basic reproduction number  $\mathcal{R}_{mz}$  is less than one, and unstable otherwise. However, the CFE may not be globally stable when  $\mathcal{R}_{mz} < 1$  due to the reinfection of malaria-infected humans with Zika virus and vice versa. This shows that bringing down the reproduction number,  $\mathcal{R}_{mz}$ , to less than one may not be enough to eradicate the coinfection of the two diseases. The effects of right and wrong treatment are also shown. It is also shown that where the two mosquitoes co-exist, an increase in the population of one of them will lead to a corresponding increase in the other, as both mosquitoes are affected by the same environmental conditions. Thus, an increase in the spread of malaria will lead to an increase in the spread of Zika virus disease as both diseases co-circulate.

**Keywords:** Malaria; Zika virus; coinfection; mis-diagnosis; wrong treatment

**AMS 2020 Classification:** 34A34; 92D30; 92B05

## 1 Introduction

Coinfection is said to be the simultaneous infection of a host by multiple pathogen species. It also includes simultaneous infection of a single cell by two or more viruses, like in the coinfection of liver cells with the hepatitis B virus and hepatitis D virus. According to [1], coinfections are certainly the norm instead of a rare occurrence. Coinfection of human immunodeficiency virus (HIV) and tuberculosis is common globally [2]. 80% of tuberculosis patients in most countries are also HIV-positive [2]. There are established cases of coinfection which include; COVID-19 and pneumonia, Hookworm and malaria, Chikungunya and Dengue, Dengue and HIV, Hepatitis C and HIV, Hepatitis C and D, COVID-19 and flu, Malaria and Zika virus, Ebola and malaria, Dengue and Zika virus, etc. [1, 3, 4]. In this work, however, we are concerned with the Malaria and Zika virus disease coinfection. The coinfection of malaria and Zika virus disease occurs when humans are bitten by infectious female Anopheles and infectious Aedes mosquitoes simultaneously and are infected by both diseases. Since the two diseases exhibit similar characteristic symptoms as shown below, the possibility of wrong diagnosis and wrong treatment of one disease as another cannot be ruled out. Also, where the two diseases co-circulate, their coinfection is possible.

Malaria is an infectious disease caused by the Plasmodium parasite and transmitted between humans through the bite of an infectious female Anopheles mosquito [5, 6]. Despite efforts at controlling this deadly disease, malaria remains highly endemic in sub-Saharan Africa and Asia, posing a threat globally. It was reported that almost half of the world's population was at risk of malaria. It is estimated that there are about 247 million cases globally, while the estimated number of deaths due to malaria was 619,000 [7]. Tropical regions in Africa accounted for 92% cases and 93% deaths, respectively, out of which Nigeria had the highest with 25% and Uganda the lowest with 4%. Symptoms of Malaria include morbidity, headache, fever, shaking chills, bloody stools, jaundice, severe anaemia, profuse sweating, nausea, muscle pain, diarrhea, vomiting, abdominal pain, fatigue, convulsions, coma, etc., [2].

Zika virus disease, as a flavivirus disease, is transmitted through the bites of infectious female Aedes mosquitoes [8, 9]. It can also be transmitted through sex, blood transfusion, or by infectious women to their newborns during pregnancy. It was reported in 2015 that over 69 countries had Zika virus infection through mosquito bites, while human-to-human transmission cases occurred in 13 countries, 29 countries had congenital transmission cases, and 20 countries had Guillain-Barre syndrome (GBs) cases [10]. Symptoms of Zika virus disease include fatigue, headache, maculopapular rash, mild fever, muscle and joint pain, retroorbital pain, oedema, vomiting, sore throat, uveitis, lymphadenopathy, malaise, arthralgia, and conjunctivitis [8, 10, 11].

There are a number of models that have analyzed the control of malaria, such as [5], whose model incorporated control strategies such as reduction of breeding sites of mosquitoes, awareness campaigns against malaria, treatment strategies, and use of insecticides. Their work showed that the control strategies were effective if sustained for a long time. [12] studied a transmission model for malaria in the Democratic Republic of Congo, incorporating optimal control measures. Their work showed that increasing the number of recovered individuals leads to a reduction in malaria cases in the future. [13] worked on the transmission dynamics of malaria disease using a nonlinear deterministic model. They used three control strategies, such as disease prevention through bed nets, treatment, and insecticides, in their optimal control analysis. [14] studied a transmission model for malaria using certain control strategies like campaign strategy for malaria control, sufficient treatment of infected people with drugs, the use of insecticide-treated bed nets, spraying of insecticides, and destruction of mosquito breeding sites, which are all capable of reducing malaria transmission. [15] worked on the optimal control of a malaria model incorporating a seasonal factor in mosquitoes. Optimal control analysis in their work showed that measures such

as the use of insecticides, prevention of breeding of mosquitoes, and treatment of infected humans will significantly reduce the spread of the disease in both human and mosquito populations simultaneously. [6] looked at the effects of temperature on the population dynamics of malaria. Their work showed that higher indoor temperature influences the efficacy of control measures. [16] considered a malaria model to prevent relapse to the disease and saturated fumigation to control the mosquitoes. Specifically, the work suggested using tafenoquine for treatment, such that when its usage is increased, the basic reproduction number decreases and vice versa. Also, [17] formulated a transmission model for malaria which incorporated the role of climatic change in the optimal control of the disease. Their optimal control showed that the use of treated bed nets, treatment of infected humans, and application of insecticides will reduce the rate of infection. [18] developed a mathematical model for the control of the spread of malaria with treatment, drug resistance, and the use of mosquito nets as control strategies. The model was fitted with data from the incidence of malaria in Nigeria. Their results showed that malaria will likely remain endemic in Nigeria except there is widespread use of mosquito nets, treatment of infectious humans is improved, and more attention is given to reducing the spread of the dominant resistant strain. [19] introduced the use of awareness campaigns against malaria, the use of insecticides and treatment as intervention measures to control the spread of malaria. The cost-effective analysis revealed that using social media to organize an awareness campaign performed better than other control measures considered in their work. [20] formulated a deterministic mathematical model to simulate the transmission of malaria between human and mosquito populations. Reducing the contact rate between humans and mosquitoes, effective treatment of infectious humans, and reducing the amount of mosquitoes in circulation were the recommendations given in his work for effective control of malaria. [21] studied a stochastic model for the control of malaria. Their work showed that the stability of the stochastic model holds more generally than a deterministic model. Mathematical modelling of Zika virus disease has been carried out by many researchers. [22] formulated a model for Zika that incorporates the use of insecticides to reduce the vectors and vaccination as control strategies. Their analysis showed that the use of indoor and outdoor insecticides increases the death rate of mosquitoes and also reduces the longevity of mosquitoes. Vaccination was also seen to play a huge role in protecting susceptible humans from contracting the virus. [23] proposed a model for Zika virus infection using delay differential equations with fractional order. The numerical simulations showed that combining fractional order and time delays in the epidemic model effectively enhances the dynamics and strengthens the stability condition of the model. [8] worked on a mathematical model that incorporated sterile-insect technology (SIT) to control the vector. Their numerical experiments showed that the release of sterile-male mosquitoes in sufficient quantity into the target population reduces the spread of mosquitoes and consequently Zika virus disease, as there are fewer vectors to transmit the disease. [24] formulated and analyzed a mathematical model for Zika virus disease, which considered both sexual and vector transmission. The model also incorporated vector control and human awareness as control measures. The model result was fitted with real data from Colombia, while they used the normalized forward sensitivity index to show that the biting rate of mosquitoes, the rate of transmission, the recruitment rate of mosquitoes, the recovery rate of humans and the awareness rate were more sensitive parameters. [25] studied the optimization of awareness campaigns and the use of insecticides against the spread of the Zika virus in human and mosquito populations. They fitted their results with real data obtained from an outbreak in Colombia and explored the various control strategies for optimality. Their work showed that combining both control strategies performed better than adopting only one of the controls. Other works modelling Zika virus disease include [9, 26, 27].

For disease coinfection, [28] worked on malaria and Zika coinfection, which highlighted the

importance of increasing the recovery rate of humans as a means of controlling the coinfection. Also, [29] carried out a study to show the impact of COVID-19 and Malaria coinfection. They conducted a cohort study with data collected from the Universal COVID-19 Treatment Center in Khartoum, Sudan. Their work showed that most patients diagnosed with COVID-19 also had malaria. [30] worked on a Zika and malaria coinfection model using a stratified survey of 100 sick persons in nine (9) secondary health centres in the southeast of Nigeria. Though no model was analyzed, blood samples of the sick persons were tested, and it was discovered that there are 20% with Zika virus, 55% with malaria, and 15% with coinfection. This study exposed the high possibility of the occurrence of both diseases. Their findings underline the need for more studies on the coinfection of malaria and Zika virus disease. [31] carried out a research study to find out the possibility of co-circulation of Zika virus with other arboviruses and malaria. Their work showed these diseases are increasingly endemic but are not well reported in some places, while also highlighting that Zika virus, malaria, and other flavivirus can co-circulate in Nigeria. [32] in their work investigated the impact of wrong treatment and misdiagnosis in the coinfection of dengue fever and Zika virus disease. Their work showed that an increase in the level of wrong treatment will lead to an increase in the total infectious population. This work attempts a similar investigation on the co-circulation and coinfection of malaria and Zika virus disease. [33] presented a mathematical model for the coinfection of malaria and Zika virus disease. Their work incorporated vaccination against malaria, treatment of infectious humans, as well as vector control through sterile-insect technology (SIT). The work established the cases of the impact of one disease on the other, attributed to misdiagnosis. The work, however, did not investigate the effect of misdiagnosis and wrong treatment. Hence, the novelty and contribution of this work are studying how misdiagnosis and wrong treatment affect the infectious classes. For further study on coinfections, see [34–36].

This work is motivated by the works of [32] and [33] as well as the works of [28, 30, 31], which have proved beyond doubt the existence of the coinfection of malaria and Zika virus disease. In this work, a new model to investigate the effects of wrong diagnoses and wrong treatment in the coinfection of malaria and Zika virus disease was presented. We aim to show that where *Anopheles* and *Aedes* mosquitoes co-exist and malaria co-circulate with Zika virus disease, then their coinfection is possible. Also, since both diseases have similar symptoms, there is a possibility of misdiagnosing one as the other and offering the wrong treatment. Then, we proceed to highlight the effect of such wrong treatment on the infected population. The rest of this work is arranged as follows: In Section 2, we present the malaria sub-model and analyze it, in Section 3, we look at the Zika sub-model with its analysis, while in Section 4, we consider the coinfection model. Numerical experiments are carried out in Section 5 while we conclude the work in Section 6.

## 2 Malaria sub-model

The Malaria sub-model is made up of seven compartments comprising the susceptible humans ( $S_h$ ), malaria infectious humans ( $I_{hm}$ ), malaria infectious humans undergoing wrong treatment due to misdiagnosis ( $T_z$ ), malaria infectious humans receiving right treatment ( $T_{hm}$ ), recovered humans ( $R_h$ ), susceptible mosquitoes ( $S_m$ ) and infectious mosquitoes ( $I_m$ ). Humans are recruited into the susceptible population at the rate  $\pi_h$  while mosquitoes are recruited into the susceptible population at the rate  $\pi_m$ . It is assumed that when mosquitoes bite humans at the rate  $\alpha_1$ , they either infect or get infected with the parasite. The parameter,  $\beta_1$  is the probability of transmission of the malaria parasite from infectious mosquitoes to humans. The malaria-infected humans,  $I_{hm}$ , malaria humans undergoing the right treatment,  $T_{hm}$  and humans wrongly treated for malaria,  $T_z$  infect the mosquitoes at the probabilities  $\beta_2$ ,  $\beta_3$  and  $\beta_4$ , respectively. Furthermore,  $\tau_1$  is the rate at which infectious humans are receiving the right treatment for malaria, and  $\tau_2$  is the rate at

which infectious humans receive wrong treatment due to misdiagnosis. Those who are not treated can recover naturally at the rate  $\phi_1$ . The rate of recovery for humans who are receiving the right treatment for malaria is  $\gamma_1$ , while the recovery rate of humans who are being treated wrongly is  $\gamma_2$ . The natural mortality rates for all humans and mosquitoes are  $\mu_h$  and  $\mu_m$ , respectively, while  $\mu_1$  is the disease-induced death rate,  $\mu_2$  is the death rate of those undergoing the right treatment, and  $\mu_3$  is the death rate due to wrong treatment. The following system of nonlinear ordinary differential equations describes the disease transmission dynamics:

$$\begin{aligned}
 \frac{dS_h(t)}{dt} &= \pi_h - \alpha_1\beta_1 I_m(t)S_h(t) - \mu_h S_h(t) + \theta R_h(t), \\
 \frac{dI_{hm}(t)}{dt} &= \alpha_1\beta_1 I_m(t)S_h(t) - (\tau_1 + \tau_2 + \phi_1 + \mu_h + \mu_1)I_{hm}(t), \\
 \frac{dT_{hm}(t)}{dt} &= \tau_1 I_{hm}(t) - (\gamma_1 + \mu_h + \mu_2)T_{hm}(t), \\
 \frac{dT_z(t)}{dt} &= \tau_2 I_{hm}(t) - (\gamma_2 + \mu_h + \mu_3)T_z(t), \\
 \frac{dR_h(t)}{dt} &= \phi_1 I_{hm}(t) + \gamma_2 T_z(t) + \gamma_1 T_{hm}(t) - (\mu_h + \theta)R_h(t), \\
 \frac{dS_m(t)}{dt} &= \pi_m - \alpha_1(\beta_2 I_{hm}(t) + \beta_3 T_{hm}(t) + \beta_4 T_z(t))S_m(t) - \mu_m S_m(t), \\
 \frac{dI_m(t)}{dt} &= \alpha_1(\beta_2 I_{hm}(t) + \beta_3 T_{hm}(t) + \beta_4 T_z(t))S_m(t) - \mu_m I_m(t),
 \end{aligned} \tag{1}$$

with the initial conditions to system (1) given as  $X_0 = (S_h^0, I_{hm}^0, T_{hm}^0, T_z^0, R_h^0, S_m^0, I_m^0)$ .

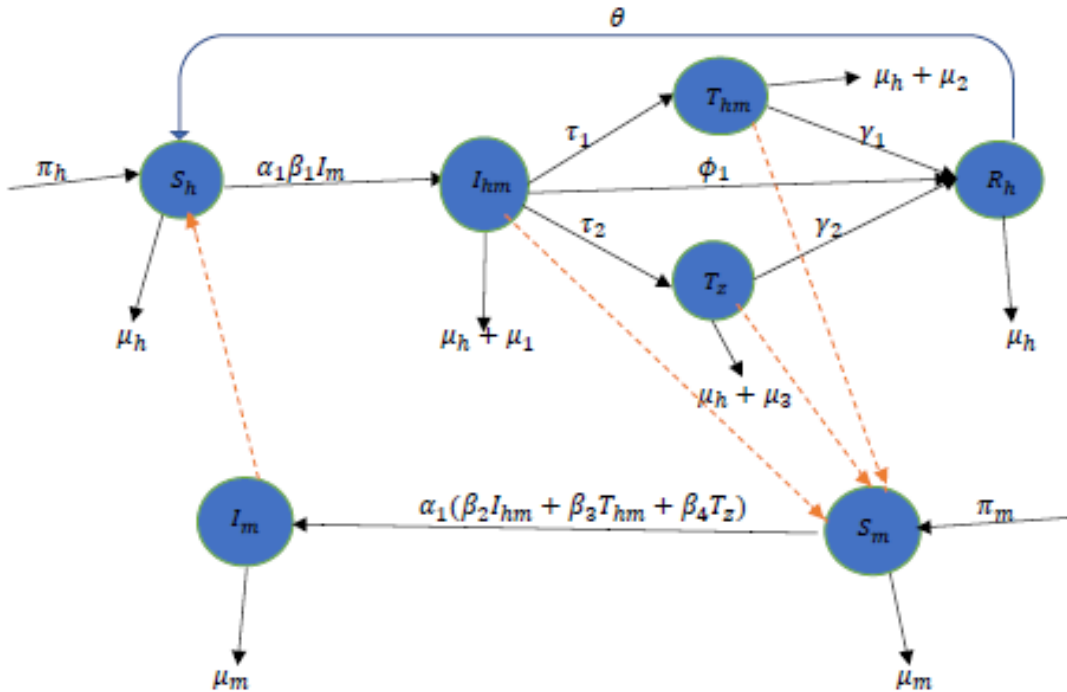


Figure 1. Malaria-only flow diagram

**Table 1.** Description of variables and parameters

Variables	Description
$S_h$	Susceptible humans
$I_{hm}$	Infectious humans with malaria
$I_{hz}$	Infectious humans with Zika virus disease
$I_{hmz}$	Coinfectious humans with both diseases
$T_{hm}$	Infectious humans with malaria undergoing right treatment
$T_{hz}$	Infectious humans with Zika undergoing right treatment
$T_m$	Infectious humans with Zika undergoing wrong treatment
$T_z$	Infectious humans with malaria undergoing wrong treatment
$T_{hmz}$	Coinfectious humans with both diseases undergoing treatment
$R_h$	Recovered humans
$S_m$	Susceptible Anopheles mosquitoes
$I_m$	Infectious Anopheles mosquitoes
$S_z$	Susceptible Aedes mosquitoes
$I_z$	Infectious Aedes mosquitoes
Parameters	Description
$\pi_h$	Level of recruitment of humans into susceptible population
$\pi_m$	Level of recruitment of Anopheles mosquitoes
$\pi_z$	Level of recruitment of Aedes mosquitoes
$\theta$	Rate of loss of immunity to malaria from recovered class
$\alpha_1$	Contact rate of Anopheles mosquitoes with humans
$\alpha_2$	Contact rate of Aedes mosquitoes with humans
$\beta_1$	Probability of transmission from infectious Anopheles mosquitoes to humans
$\beta_2$	Probability of transmission from infectious humans to Anopheles mosquitoes
$\beta_3$	Probability of transmission from humans undergoing treatment to Anopheles mosquitoes
$\beta_4$	Probability of transmission from humans undergoing wrong treatment to Anopheles mosquitoes
$\eta_1$	Probability of transmission from infectious Aedes mosquitoes to humans
$\eta_2$	Probability of transmission from infectious humans to Aedes mosquitoes
$\eta_3$	Probability of transmission from humans undergoing treatment to Aedes mosquitoes
$\eta_4$	Probability of transmission from humans undergoing wrong treatment to Aedes mosquitoes
$\mu_h$	Natural death rate of humans
$\mu_m$	Natural death rate of mosquitoes
$\mu_1$	Disease-induced death rate in infectious humans with malaria only
$\mu_2$	Disease-induced death rate in infectious humans with malaria only undergoing right treatment
$\mu_3$	Disease-induced death rate in infectious humans with malaria only undergoing wrong treatment
$\mu_4$	Disease-induced death rate in infectious humans with Zika only
$\mu_5$	Disease-induced death rate in infectious humans with Zika only undergoing right treatment
$\mu_6$	Disease-induced death rate in infectious humans with Zika only undergoing wrong treatment
$\mu_7$	Disease-induced death rate in coinfectious humans
$\mu_8$	Disease-induced death rate in coinfectious humans undergoing treatment
$\tau_1$	Rate at which infectious humans with malaria undergo the right treatment
$\tau_2$	Rate at which infectious humans with malaria undergo the wrong treatment
$\tau_3$	Rate at which infectious humans with Zika undergo the right treatment
$\tau_4$	Rate at which infectious humans with Zika undergo the wrong treatment
$\tau_5$	Rate at which coinfectious humans undergo treatment for both diseases
$\tau_6$	Rate at which coinfectious humans undergo treatment for only malaria

$\tau_7$	Rate at which coinfectious humans undergo treatment for only Zika virus
$\gamma_1$	Rate of recovery of infectious humans with malaria undergoing the right treatment
$\gamma_2$	Rate of recovery of infectious humans with malaria undergoing wrong treatment
$\gamma_3$	Rate of recovery of infectious humans with Zika undergoing the right treatment
$\gamma_4$	Rate of recovery of infectious humans with Zika undergoing wrong treatment
$\gamma_5$	Rate of recovery of coinfectious humans undergoing treatment
$\phi_1$	Rate at which infectious humans with malaria not undergoing treatment
$\phi_2$	Rate at which infectious humans with Zika virus not undergoing treatment

**Positivity of solutions and invariant region**

**Lemma 1** *Given that the initial conditions  $(S_h^0, I_{hm}^0, T_{hm}^0, T_z^0, R_h^0, S_m^0, I_m^0) > 0$  at  $t = 0$  lies in the region,  $\Omega$ , then the solution set  $(S_h(t), I_{hm}(t), T_{hm}(t), T_z(t), R_h(t), S_m(t), I_m(t))$  to the system remains positive  $\forall t > 0$ .*

**Proof** We see from the first and second equation in (1) that

$$\begin{aligned} \frac{dS_h(t)}{dt} &\geq -(\alpha_1\beta_1I_m(t) + \mu_h)S_h(t), \quad \text{and} \\ \frac{dI_{hm}(t)}{dt} &\geq -(\tau_1 + \tau_2 + \phi_1 + \mu_h + \mu_1)I_{hm}(t), \end{aligned}$$

which we solve to get

$$\begin{aligned} S_h(t) &\geq S_h^0 e^{-\int_0^t (\alpha_1\beta_1I_m(t) + \mu_h) dt} > 0, \quad \text{and} \\ I_{hm}(t) &\geq I_{hm}^0 e^{-(\tau_1 + \tau_2 + \phi_1 + \mu_h + \mu_1)t} > 0, \end{aligned}$$

respectively. Therefore, the solutions  $S_h(t)$  and  $I_{hm}(t)$  will remain positive for all  $t$  with the given positive initial conditions. Similar results can be obtained for the other components. Hence, the solution to the model system remains positive at all times provided the initial solution set is positive [37, 38].

**Lemma 2** *Every solution to the system (1) lies within the region  $\Omega$ . That is, the region  $\Omega$  is bounded.*

**Proof** We want to prove that the region,  $\Omega$  is positively invariant by showing that all the solutions to the model system will enter and remain in  $\Omega$ . Let  $(S_h, I_{hm}, T_{hm}, T_z, R_h) \in \mathbb{R}^5$ , be the solution to the human component of the system, with positive initial values and  $(S_m, I_m) \in \mathbb{R}^2$ . It can be shown that the total human and mosquito populations satisfy the differential equations

$$\begin{aligned} \frac{dN_h}{dt} &= \pi_h - \mu_h N_h - N_1, \\ \frac{dN_m}{dt} &= \pi_m - \mu_m N_m, \end{aligned} \tag{2}$$

respectively, where  $N_1 = \mu_1 I_{hm} + \mu_2 T_{hm} + \mu_3 T_z$ . Then, from (2), we have  $\frac{dN_h(t)}{dt} \leq \pi_h - \mu_h N_h(t)$ , whose solution is  $N_h(t) \leq \frac{\pi_h}{\mu_h} + \left(N(0) - \frac{\pi_h}{\mu_h}\right) e^{-\mu_h t}$ . This shows that as  $t \rightarrow \infty$ , we have  $0 < N_h \leq \frac{\pi_h}{\mu_h}$ . Thus, all feasible solutions to the human-only component of the model system enter and remain in the region  $\Omega_h = \left\{ (S_h, I_{hm}, T_{hm}, T_z, R_h) \in \mathbb{R}^5 : N_h \leq \frac{\pi_h}{\mu_h} \right\}$ .

Using the same procedure, we can show that all feasible solutions to the mosquito components of the equation enter and remain in the region  $\Omega_m = \left\{ (S_m, I_m) \in \mathbb{R}^2 : N_m \leq \frac{\pi_m}{\mu_m} \right\}$ . Thus, all possible

solutions to the system will remain bounded in the region  $\Omega = \Omega_h \times \Omega_m$  and prove that the region  $\Omega$  is positively invariant with respect to the flow generated by (1). The results of Lemma 1 and Lemma 2 are sufficient conditions to consider and analyze the system in this feasible region  $\Omega$  because it is epidemiologically and mathematically well-posed in the region, hence can be studied and analyzed [4, 39, 40].

### Malaria basic reproduction number

The malaria-free equilibrium point (MFE) is the steady state solution of (1) where there is no malaria in the system [41, 42]. It is obtained by equating  $I_{hm} = T_{hm} = T_z = I_m = 0$  and solving to obtain the values of state variables. Thus, the malaria-free equilibrium point denoted here by  $E_m^0$  is given by  $E_m^0 = \left( \frac{\pi_h}{\mu_h}, 0, 0, 0, 0, \frac{\pi_m}{\mu_m}, 0 \right)$ .

The malaria basic reproduction number,  $\mathcal{R}_{0m}$  is the average number of new cases of malaria that can be caused by one new infectious case of the disease introduced into an entirely susceptible population [33]. This important threshold number is calculated using the next-generation matrix approach. The malaria basic reproduction number is calculated as the spectral radius of the Next-Generation matrix ( $F_{0m}V_{0m}^{-1}$ ), where  $F_{0m}$  and  $V_{0m}$  are the Jacobian matrices obtained from the diseased classes in the system [43, 44]. The matrices of  $F_{0m}$  and  $V_{0m}$  are given as

$$F_{0m} = \begin{pmatrix} 0 & 0 & 0 & A_1 \\ 0 & 0 & 0 & 0 \\ 0 & 0 & 0 & 0 \\ A_2 & A_3 & A_4 & 0 \end{pmatrix}, \text{ and } V_{0m} = \begin{pmatrix} B_1 & 0 & 0 & 0 \\ -\tau_1 & B_2 & 0 & 0 \\ -\tau_2 & 0 & B_3 & 0 \\ 0 & 0 & 0 & \mu_m \end{pmatrix},$$

where  $A_1 = \frac{\alpha_1\beta_1\pi_h}{\mu_h}$ ,  $A_2 = \frac{\alpha_1\beta_2\pi_m}{\mu_m}$ ,  $A_3 = \frac{\alpha_1\beta_3\pi_m}{\mu_m}$ ,  $A_4 = \frac{\alpha_1\beta_4\pi_m}{\mu_m}$ ,  $B_1 = \tau_1 + \tau_2 + \phi_1 + \mu_1 + \mu_h$ ,  $B_2 = \gamma_1 + \mu_h + \mu_2$ ,  $B_3 = \gamma_2 + \mu_h + \mu_3$ . The Next-Generation matrix is obtained to be

$$F_{0m}V_{0m}^{-1} = \begin{pmatrix} 0 & 0 & 0 & \frac{A_1}{\mu_m} \\ 0 & 0 & 0 & 0 \\ 0 & 0 & 0 & 0 \\ \frac{A_2}{B_1} + \frac{A_3\tau_1}{B_1B_2} + \frac{A_4\tau_2}{B_1B_3} & \frac{A_3}{B_2} & \frac{A_4}{B_3} & 0 \end{pmatrix},$$

with the eigenvalues  $0, 0, \pm \sqrt{\frac{A_1(A_2B_2B_3 + A_3\tau_1B_3 + A_4\tau_2B_2)}{\mu_m B_1 B_2 B_3}}$ . Therefore, the malaria basic reproduction number is

$$\mathcal{R}_{0m} = \sqrt{\frac{A_1(A_2B_2B_3 + A_3\tau_1B_3 + A_4\tau_2B_2)}{\mu_m B_1 B_2 B_3}}, \quad (3)$$

which can be rewritten as

$$\mathcal{R}_{0m}^2 = \frac{A_1A_2}{\mu_m B_1} + \frac{A_1\tau_1A_3}{\mu_m B_1 B_2} + \frac{A_1\tau_2A_4}{\mu_m B_1 B_3}. \quad (4)$$

The term  $\frac{A_1A_2}{\mu_m B_1}$  in (4) is the total expected number of humans that will be infected at the malaria-free equilibrium point by a single newly infected human whilst they are infectious but before entering treatment,  $\frac{A_1\tau_1A_3}{\mu_m B_1 B_2}$  is the total expected number of humans that will be infected at the malaria-free equilibrium point by a single newly infected human whilst they are undergoing right

treatment for malaria while  $\frac{A_1\tau_2A_4}{\mu_m B_1 B_3}$  is the total expected number of humans that will be infected at the malaria-free equilibrium point by a single newly infected human whilst they are undergoing incorrect treatment for malaria.

**Local asymptotic stability of malaria-free equilibrium point**

**Theorem 1** *The malaria-free equilibrium point is locally asymptotically stable if  $\mathcal{R}_{0m} < 1$ , and unstable if  $\mathcal{R}_{0m} > 1$ .*

**Proof** The Jacobian matrix of malaria sub-model evaluated at the malaria-free equilibrium point is

$$J(E_m^0) = \begin{pmatrix} -\mu_h & 0 & 0 & 0 & \theta & 0 & -A_1 \\ 0 & -B_1 & 0 & 0 & 0 & 0 & A_1 \\ 0 & \tau_1 & -B_2 & 0 & 0 & 0 & 0 \\ 0 & \tau_2 & 0 & -B_3 & 0 & 0 & 0 \\ 0 & 0 & \gamma_1 & \gamma_2 & -B_4 & 0 & 0 \\ 0 & -A_2 & -A_3 & -A_4 & 0 & -\mu_m & 0 \\ 0 & A_2 & A_3 & A_4 & 0 & 0 & -\mu_m \end{pmatrix},$$

with  $B_4 = \theta + \mu_h$  and all the  $A_i$ 's and  $B_i$ 's are the same as in Section 2. The Jacobian matrix,  $J(E_m^0)$  can be reduced to a submatrix if the rows and the columns with one entry are removed. The eigenvalues of the system corresponds to  $-\mu_h, -\mu_m, -(\mu_h + \theta)$  and the eigenvalues of the submatrix

$$J_1(E_m^0) = \begin{pmatrix} -B_1 & 0 & 0 & A_1 \\ \tau_1 & -B_2 & 0 & 0 \\ \tau_2 & 0 & -B_3 & 0 \\ A_2 & A_3 & A_4 & -\mu_m \end{pmatrix}.$$

The characteristics polynomial that corresponds to the submatrix,  $J_1(E_m^0)$  is given by

$$P(\lambda) = \lambda^4 + Q_3\lambda^3 + Q_2\lambda^2 + Q_1\lambda + Q_0, \tag{5}$$

where

$$\begin{aligned} Q_3 &= \mu_m + B_1 + B_2 + B_3, \\ Q_2 &= \mu_m(B_2 + B_3) + B_1(B_2 + B_3) + B_2B_3 + \frac{A_1\tau_1A_3}{B_2} + \frac{A_1\tau_2A_4}{B_3} + \mu_mB_1[1 - R_{0m}^2], \\ Q_1 &= B_1B_2(\mu_m + B_3) + \frac{A_1\tau_1A_3B_3}{B_2} + \frac{A_1\tau_2A_4B_2}{B_3} + \mu_mB_1(B_2 + B_3)[1 - R_{0m}^2], \\ Q_0 &= \mu_mB_1B_2B_3[1 - R_{0m}^2]. \end{aligned}$$

According to [45, 46], Routh-Hurwitz criterion for stability states that all roots of the characteristic polynomial  $P(\lambda)$  will have negative real parts if  $Q_3 > 0, Q_2 > 0, Q_1 > 0, Q_0 > 0$  and  $Q_3Q_2 > Q_1$ . These conditions are satisfied if  $R_{0m} < 1$ . This shows that  $E_m^0$  is locally asymptotically stable if  $\mathcal{R}_{0m} < 1$ , and unstable if  $\mathcal{R}_{0m} > 1$ . Hence, if  $\mathcal{R}_{0m} < 1$ , then malaria can die out in the system depending on the initial size of the infected population.

### Global asymptotic stability of malaria-free equilibrium point

The method of Castillo-Chavez [47] summarized in Lemma 3 below, was employed to check if the MFE is globally asymptotically stable (GAS) or not.

**Lemma 3** Consider the system of differential equations

$$\frac{dX_1}{dt} = F_1(X_1, 0), \quad (6)$$

$$\frac{dX_2}{dt} = F_2(X_1, X_2), F_2(X_1, 0) = 0, \quad (7)$$

where (6) is the system of differential equations, satisfied by non-diseased classes such that  $X_1 = (S_h, R_h, S_m)$  and (7) is the system of differential equations satisfied by the diseased classes so that  $X_2 = (I_{hm}, T_{hm}, T_z, I_m)$ . The malaria-free equilibrium point (MFE),  $E_m^0$  is globally asymptotically stable if (6) is globally asymptotically stable, and if in (7),  $BX_2 - F_1(X_1, X_2) = 0$ , where  $B$  is the Jacobian matrix of  $F_2(X_1, X_2)$ , evaluated at  $E_m^0$ .

**Theorem 2** The malaria-free equilibrium point of the model (1) is globally asymptotic stable if  $\mathcal{R}_{0m} < 1$  and unstable if  $\mathcal{R}_{0m} > 1$ .

**Proof** We only need to employ Lemma 3 and show that the conditions on (6) and (7) holds if  $\mathcal{R}_{0m} < 1$ . At the malaria-free equilibrium point, the corresponding differential equations for  $X_1 = (S_h, R_h, S_m)$ , taking note that  $I_{hm} = T_{hm} = T_z = R_h = 0$ , become

$$\begin{aligned} \frac{dS_h(t)}{dt} &= \pi_h - \mu_h S_h(t), \\ \frac{dR_h(t)}{dt} &= 0, \\ \frac{dS_m(t)}{dt} &= \pi_m - \mu_m S_m(t). \end{aligned} \quad (8)$$

Solving the resulting differential equations of (7) by integration gives

$$\begin{aligned} S_h(t) &= \frac{\pi_h}{\mu_h} + (S_h^0 - \frac{\pi_h}{\mu_h})e^{-\mu_h t}, \\ R_h(t) &= R_h^0 = 0, \\ S_m(t) &= \frac{\pi_m}{\mu_m} + \left(S_m^0 - \frac{\pi_m}{\mu_m}\right)e^{-\mu_m t}. \end{aligned} \quad (9)$$

As  $t \rightarrow \infty$ , we will have  $S_h \rightarrow \frac{\pi_h}{\mu_h}$ ,  $R_h \rightarrow 0$  and  $S_m \rightarrow \frac{\pi_m}{\mu_m}$  respectively which corresponds to the values of these state variables at the MFE. Thus, (6) is GAS.

Also, the matrix  $B$  corresponds to our Jacobian submatrix,  $J_1(E_m^0)$ . Hence, the expression  $BX_2 - F_1(X_1, X_2)$  becomes

$$BX_2 - F_1(X_1, X_2) = \begin{pmatrix} \alpha_1 \beta_1 \left(\frac{\pi_h}{\mu_h} - S_h\right) I_m \\ 0 \\ 0 \\ \alpha_1 (\beta_2 I_{hm} + \beta_3 T_{hm} + \beta_4 T_z) \left(\frac{\pi_m}{\mu_m} - S_m\right) \end{pmatrix}.$$

Since  $S_h \rightarrow \frac{\pi_h}{\mu_h}$ , and  $S_m \rightarrow \frac{\pi_m}{\mu_m}$  then,  $\frac{\pi_h}{\mu_h} \geq S_h$  and  $\frac{\pi_m}{\mu_m} \geq S_m$  respectively. Thus,  $BX_2 - G(X_1, X_2) \geq 0$ . Hence, the malaria-free equilibrium point is globally asymptotical stable. This shows that the model has a unique endemic equilibrium which exists if  $\mathcal{R}_{0m} > 1$ . This rules out the possible occurrence of backward bifurcation in the model, since backward bifurcation requires at least two endemic equilibria to occur. Epidemiologically, this means that having  $\mathcal{R}_{0m} < 1$  is a necessary and sufficient condition for eradicating malaria in the population [48].

### Endemic equilibrium point of the malaria-only model

The malaria endemic equilibrium points (MEEPs) are steady-state solutions in the population where malaria persists, that is, where all state variables are positive. The malaria endemic equilibrium point is denoted in this work by  $E_m^* = (S_h^*, I_{hm}^*, T_{hm}^*, T_z^*, R_h^*, S_m^*, I_m^*)$  and expressed in terms of  $I_{hm}^*$ . Thus we have

$$S_h^* = \frac{(\pi_h + f_4 I_{hm}^*) [f_1 I_{hm}^* + f_2]}{\alpha_1 \beta_1 f_3 \mathcal{R}_{0m}^2 I_{hm}^* + \mu_h [f_1 I_{hm}^* + f_2]}, T_{hm}^* = \frac{\tau_1 I_{hm}^*}{B_2}, T_z^* = \frac{\tau_2 I_{hm}^*}{B_3}, R_h^* = f_4 I_{hm}^*,$$

$$S_m^* = \frac{\pi_m B_2 B_3}{f_1 I_{hm}^* + f_2}, I_m^* = \frac{f_3 \mathcal{R}_{0m}^2 I_{hm}^*}{f_1 I_{hm}^* + f_2},$$

where  $B_4 = \mu_h + \theta$ ,  $f_1 = \alpha_1 \beta_2 B_2 B_3 + \alpha_1 \beta_3 \tau_1 B_3 + \alpha_1 \beta_4 \tau_2 B_2$ ,  $f_2 = \mu_m B_2 B_3$ ,  $f_3 = \frac{\mu_m B_1 B_2 B_3}{A_1}$ ,

$f_4 = \frac{B_3 \gamma_1 \tau_1 + B_2 \gamma_2 \tau_2}{B_2 B_3 B_4}$  with the other  $A_i$ 's and  $B_i$ 's same as in Section 2. In the above expressions for the state variables at the endemic points, if we set  $I_{hm}^* = 0$ , we could see that all the state variables  $(S_h, I_{hm}, T_{hm}, R_h, S_m, I_m) \rightarrow (\frac{\pi_h}{\mu_h}, 0, 0, 0, 0, \frac{\pi_m}{\mu_m}, 0)$  which corresponds to the malaria-free equilibrium point. When  $I_{hm}^* \neq 0$ , we have the endemic equilibrium point for the malaria sub-model.

**Theorem 3** *The malaria endemic equilibrium point exists and is unique if  $\mathcal{R}_{0m} > 1$ .*

**Proof** Substituting the values for the state variables into the equation for  $I_{hm}^*$  in (1) gives;

$$\mathcal{G}_1 I_{hm}^{*2} + \mathcal{G}_2 I_{hm}^* = 0, \tag{10}$$

where  $\mathcal{G}_1 = A_1 f_3 (B_1 - f_4) \mathcal{R}_{0m}^2 + \pi_h f_1 B_1$  and  $\mathcal{G}_2 = \mu_m B_1 B_2 B_3 \pi_h (1 - \mathcal{R}_{0m}^2)$ .

**Case 1:** If  $\mathcal{G}_1 > 0$  and  $\mathcal{G}_2 < 0$ , a unique endemic equilibrium point exists at  $\mathcal{R}_{0m} > 1$ .

**Case 2:** If  $\mathcal{G}_1 > 0$  and  $\mathcal{G}_2 > 0$ , then  $\mathcal{R}_{0m} < 1$  and no endemic equilibrium point will exist.

**Case 3:** Similarly, if  $\mathcal{G}_1 < 0$  and  $\mathcal{G}_2 < 0$ , then no endemic equilibrium point will exist at  $\mathcal{R}_{0m} > 1$ .

**Case 4:** If  $\mathcal{G}_1 < 0$  and  $\mathcal{G}_2 > 0$ , then an endemic equilibrium point exists when  $\mathcal{R}_{0m} < 1$ . This situation cannot be regarded as backward bifurcation since the latter occurs for more than one endemic equilibrium point. Hence, the endemic equilibrium point for the malaria sub-model exists when  $\mathcal{R}_{0m} > 1$ .

### 3 Zika sub-model

The Zika disease sub-model is made up of seven compartments: the susceptible humans  $S_h$ , Zika infectious humans  $I_{hz}$ , Zika infectious humans receiving wrong treatment due to misdiagnosis  $T_m$ , Zika infectious humans receiving right treatment  $T_{hz}$ , recovered humans  $R_h$ , susceptible mosquitoes  $S_z$  and infectious mosquitoes with Zika,  $I_z$ . The level of recruitment of humans into the susceptible class is  $\pi_h$ . The infectious mosquitoes bite humans at the rate  $\alpha_2$  and transmit Zika virus with probability  $\eta_1$ . We assume that the rate at which Zika-infected humans receive the right treatment is  $\tau_3$ , while the rate of receiving wrong treatment due to misdiagnosis is  $\tau_4$ .

The rates of recovery for  $T_{hz}$  and  $T_m$  are put at  $\gamma_3$  and  $\gamma_4$ , respectively. The untreated humans in  $I_{hz}$  recover at the rate,  $\phi_2$ . Also,  $\mu_h$  and  $\mu_z$  are the natural mortality rates for humans and mosquitoes, respectively, while  $\mu_4$ ,  $\mu_5$  and  $\mu_6$  are the disease-induced death rates for infectious humans, humans undergoing treatment for Zika, and humans wrongly treated, respectively. In the mosquito population, the level of recruitment of mosquitoes into the susceptible class is  $\pi_z$ . The susceptible class of mosquitoes contracts Zika virus with the probabilities  $\eta_2$ ,  $\eta_3$  and  $\eta_4$  respectively, when they bite humans in the infectious classes  $I_{hz}$ ,  $T_{hz}$  and  $T_m$  at the biting rate  $\alpha_2$ . The above assumptions on the transmission dynamics of Zika lead to the following system of nonlinear ordinary differential equations:

$$\begin{aligned}
 \frac{dS_h(t)}{dt} &= \pi_h - \alpha_2 \eta_1 I_z(t) S_h(t) - \mu_h S_h(t), \\
 \frac{dI_{hz}(t)}{dt} &= \alpha_2 \eta_1 I_z(t) S_h(t) - (\tau_3 + \tau_4 + \phi_2 + \mu_h + \mu_4) I_{hz}(t), \\
 \frac{dT_{hz}(t)}{dt} &= \tau_3 I_{hz}(t) - (\gamma_3 + \mu_h + \mu_5) T_{hz}(t), \\
 \frac{dT_m(t)}{dt} &= \tau_4 I_{hz}(t) - (\gamma_4 + \mu_h + \mu_6) T_m(t), \\
 \frac{dR_h(t)}{dt} &= \phi_2 I_{hz}(t) + \gamma_3 T_{hz}(t) + \gamma_4 T_m(t) - \mu_h R_h(t), \\
 \frac{dS_z(t)}{dt} &= \pi_z - \alpha_2 (\eta_2 I_{hz}(t) + \eta_3 T_{hz}(t) + \eta_4 T_m(t)) S_z(t) - \mu_z S_z(t), \\
 \frac{dI_z(t)}{dt} &= \alpha_2 (\eta_2 I_{hz}(t) + \eta_3 T_{hz}(t) + \eta_4 T_m(t)) S_z(t) - \mu_z I_z(t),
 \end{aligned}
 \tag{11}$$

with the initial conditions to the system (11) given as  $Y_0 = (S_h^0, I_{hz}^0, T_{hz}^0, T_m^0, R_h^0, S_z^0, I_z^0)$ .

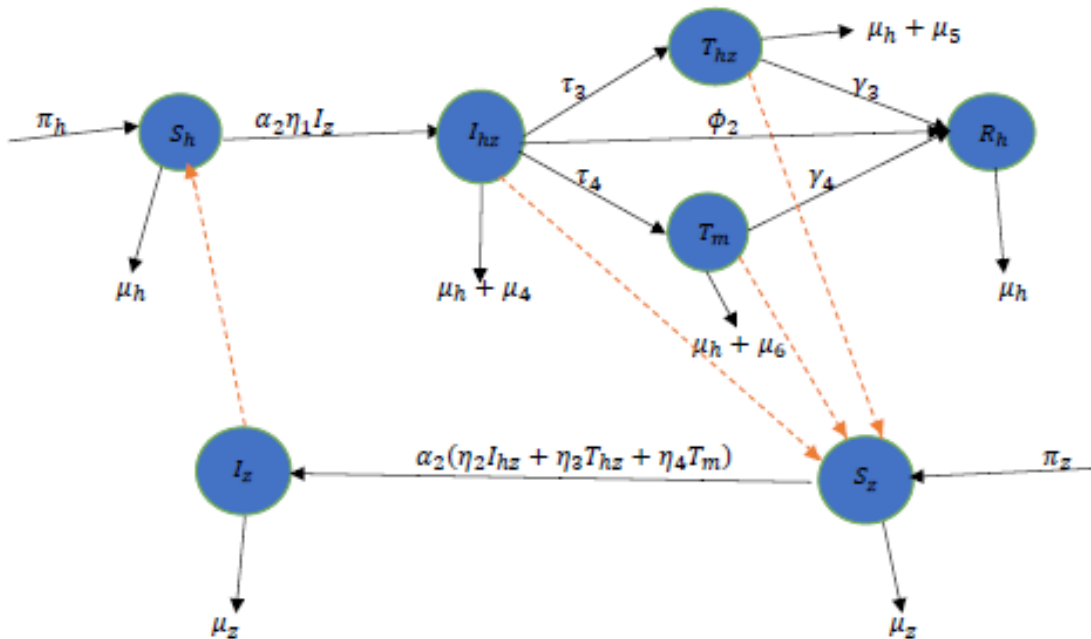


Figure 2. Zika-only flow diagram

### Positivity of solutions and invariant region

The positivity of solutions to the Zika sub-model can be established using the same procedure for the malaria sub-model and shown to be positive at all times. Also, all feasible solutions to the human and mosquito components of the equation enter and remain in the region  $\Omega_h = \left\{ (S_h, I_{hz}, T_{hz}, T_m, R_h) \in \mathbb{R}^5 : N_h \leq \frac{\pi_h}{\mu_h} \right\}$  and  $\Omega_z = \left\{ (S_z, I_z) \in \mathbb{R}^2 : N_z \leq \frac{\pi_z}{\mu_z} \right\}$  respectively. Thus, all possible solutions to the system will remain bounded in the region  $\Omega = \Omega_h \times \Omega_z$  and prove that the region  $\Omega$  is positively invariant with respect to the flow generated by (11). Thus, the system is epidemiologically well-posed in the region [39].

### Zika-free equilibrium point and basic reproduction number of Zika

The zika-free equilibrium point is given by  $E_z^0 = \left( \frac{\pi_h}{\mu_h}, 0, 0, 0, 0, \frac{\pi_z}{\mu_z}, 0 \right)$  and the Next-Generation matrix for Zika sub-model, following the same procedure as that of malaria, is

$$F_{0z}V_{0z}^{-1} = \begin{pmatrix} 0 & 0 & 0 & 0 & \frac{C_1}{\mu_z} \\ 0 & 0 & 0 & 0 & 0 \\ 0 & 0 & 0 & 0 & 0 \\ \frac{C_2}{D_1} + \frac{C_3\tau_3}{D_1D_2} + \frac{C_4\tau_4}{D_1D_3} & \frac{C_3}{D_2} & \frac{C_4}{D_3} & 0 & 0 \end{pmatrix},$$

where  $C_1 = \frac{\alpha_2\eta_1\pi_h}{\mu_h}, C_2 = \frac{\alpha_2\eta_2\pi_z}{\mu_z}, C_3 = \frac{\alpha_2\eta_3\pi_z}{\mu_z}, C_4 = \frac{\alpha_2\eta_4\pi_z}{\mu_z}, D_1 = \tau_3 + \tau_4 + \phi_2 + \mu_4 + \mu_h,$   
 $D_2 = \gamma_3 + \mu_h + \mu_5, D_3 = \gamma_4 + \mu_h + \mu_6.$

The eigenvalues of the next-generation matrix,  $F_{0z}V_{0z}^{-1}$  is

$$\left( 0, 0, \pm \sqrt{\frac{C_1(C_2D_2D_3 + C_3\tau_3D_3 + C_4\tau_4D_2)}{\mu_zD_1D_2D_3}} \right).$$

Therefore, the Zika control number is

$$\mathcal{R}_{0z} = \sqrt{\frac{C_1(C_2D_2D_3 + C_3\tau_3D_3 + C_4\tau_4D_2)}{\mu_zD_1D_2D_3}}, \tag{12}$$

which can be rewritten as

$$\mathcal{R}_{0z}^2 = \frac{C_1C_2}{\mu_zD_1} + \frac{C_1\tau_3C_3}{\mu_zD_1D_2} + \frac{C_1\tau_4C_4}{\mu_zD_1D_3}.$$

The term  $\frac{C_1C_2}{\mu_zD_1}$ , in (12) is the total expected population of humans that will be infected at the Zika-free equilibrium point by one newly infectious human before entering treatment,  $\frac{C_1\tau_3C_3}{\mu_zD_1D_2}$  is the total expected number of humans that will be infected at the Zika-free equilibrium point by one newly infectious human whilst they are undergoing treatment for Zika while  $\frac{C_1\tau_4C_4}{\mu_zD_1D_3}$  is the total expected number of humans that will be infected at the Zika-free equilibrium point by one newly infectious human whilst they are undergoing incorrect treatment for Zika.

### Local asymptotic stability of the Zika-free equilibrium point

**Theorem 4** *The Zika-free equilibrium point is locally asymptotically stable if  $\mathcal{R}_{0z} < 1$ , and unstable if  $\mathcal{R}_{0z} > 1$ .*

The Jacobian matrix of the Zika sub-model evaluated at the Zika-free equilibrium point is

$$J(E_z^0) = \begin{pmatrix} -\mu_h & 0 & 0 & 0 & 0 & 0 & -C_1 \\ 0 & -D_1 & 0 & 0 & 0 & 0 & C_1 \\ 0 & \tau_3 & -D_2 & 0 & 0 & 0 & 0 \\ 0 & \tau_4 & 0 & -D_3 & 0 & 0 & 0 \\ 0 & 0 & \gamma_3 & \gamma_4 & -\mu_h & 0 & 0 \\ 0 & -C_2 & -C_3 & -C_4 & 0 & -\mu_z & 0 \\ 0 & C_2 & C_3 & C_4 & 0 & 0 & -\mu_z \end{pmatrix}.$$

The eigenvalues of the Jacobian matrix,  $J(E_z^0)$  are  $-\mu_h, -\mu_h, -\mu_z$ , and the eigenvalues of the sub-matrix

$$J_1(E_z^0) = \begin{pmatrix} -D_1 & 0 & 0 & C_1 \\ \tau_3 & -D_2 & 0 & 0 \\ \tau_4 & 0 & -D_3 & 0 \\ C_2 & C_3 & C_4 & -\mu_z \end{pmatrix}.$$

The submatrix,  $-J_1(E_z^0)$ , is similar to the Jacobian submatrix,  $J_1(E_m^0)$  obtained in (2.3). This implies that all the eigenvalues of  $J_1(E_z^0)$  are negative or have a negative real part if  $\mathcal{R}_{0z} < 1$ . Therefore, the zika-free equilibrium point,  $E_z^0$  is locally asymptotically stable if  $\mathcal{R}_{0z} < 1$ , and unstable if  $\mathcal{R}_{0z} > 1$ .

### Global asymptotic stability of Zika-free equilibrium point

Following the same procedure used in establishing the global stability of the malaria-free equilibrium, the corresponding differential equations for  $Y_1 = (S_h, R_h, S_z)$ , taking note that  $I_{hz} = T_{hz} = T_m = R_h = 0$ , become

$$\begin{aligned} \frac{dS_h(t)}{dt} &= \pi_h - \mu_h S_h(t), \\ \frac{dR_h(t)}{dt} &= 0, \\ \frac{dS_z(t)}{dt} &= \pi_z - \mu_z S_z(t). \end{aligned} \tag{13}$$

Solving the resulting differential equations of (7) by integration gives

$$\begin{aligned} S_h(t) &= \frac{\pi_h}{\mu_h} + (S_h^0 - \frac{\pi_h}{\mu_h})e^{-\mu_h t}, \\ R_h(t) &= R_h^0 = 0, \\ S_z(t) &= \frac{\pi_z}{\mu_z} + \left(S_z^0 - \frac{\pi_z}{\mu_z}\right)e^{-\mu_z t}. \end{aligned} \tag{14}$$

As  $t \rightarrow \infty$ , we will have  $S_h \rightarrow \frac{\pi_h}{\mu_h}$ ,  $R_h \rightarrow 0$  and  $S_z \rightarrow \frac{\pi_z}{\mu_z}$  respectively which corresponds to the values of these state variables at the ZFE. Thus, (6) is GAS.

Also, the matrix  $B$  corresponds to our Jacobian submatrix,  $J_1(E_z^0)$ . Hence, the expression  $BX_2 - F_1(X_1, X_2)$  becomes

$$BX_2 - F_1(X_1, X_2) = \begin{pmatrix} \alpha_1\beta_1\left(\frac{\pi_h}{\mu_h} - S_h\right)I_z \\ 0 \\ 0 \\ \alpha_2(\eta_2I_{hz} + \eta_3T_{hz} + \eta_4T_m)\left(\frac{\pi_z}{\mu_z} - S_z\right) \end{pmatrix}.$$

Since  $S_h \rightarrow \frac{\pi_h}{\mu_h}$ , and  $S_z \rightarrow \frac{\pi_z}{\mu_z}$  then,  $\frac{\pi_h}{\mu_h} \geq S_h$  and  $\frac{\pi_z}{\mu_z} \geq S_z$  respectively. Thus,  $BX_2 - G(X_1, X_2) \geq 0$ . Hence, the Zika-free equilibrium point is globally asymptotical stable. This shows that the model has a unique endemic equilibrium which exists if  $\mathcal{R}_{0z} > 1$ . This rules out the possible occurrence of backward bifurcation in the model, since backward bifurcation requires at least two endemic equilibria to occur. Epidemiologically, this means that having  $\mathcal{R}_{0z} < 1$  is a necessary and sufficient condition for eradicating Zika virus disease in the population.

### Endemic equilibrium point of the Zika sub-model

The Zika endemic equilibrium point is a steady-state solution in the population where Zika persists, that is, where all state variables are positive. The Zika endemic equilibrium points denoted in this work by  $E_z^* = (S_h^*, I_{hz}^*, T_{hz}^*, T_m^*, R_h^*, S_z^*, I_z^*)$  is gotten in terms of  $I_{hz}^*$  as

$$S_h^* = \frac{\pi_h[g_1I_{hz}^* + g_2]}{\alpha_2\eta_1g_3\mathcal{R}_{0z}^2I_{hz}^* + \mu_h[g_1I_{hz}^* + g_2]}, T_{hz}^* = \frac{\tau_3I_{hz}^*}{D_2}, T_m^* = \frac{\tau_4I_{hz}^*}{D_3}, R_h^* = g_4I_{hz}^*, S_z^* = \frac{\pi_zD_2D_3}{g_1I_{hz}^* + g_2},$$

$$I_z^* = \frac{g_3\mathcal{R}_{0z}^2I_{hz}^*}{g_1I_{hz}^* + g_2}, \text{ where } g_1 = \alpha_2\eta_2D_2D_3 + \alpha_2\eta_3\tau_3D_3 + \alpha_2\eta_4\tau_4D_2, g_2 = \mu_zD_2D_3, g_3 = \frac{\mu_zD_1D_2D_3}{C_1},$$

$$\text{and } g_4 = \frac{D_3\gamma_3\tau_3 + D_2\gamma_4\tau_4}{\mu_hD_2D_3}.$$

**Theorem 5** *The Zika endemic equilibrium point exist and is unique if  $\mathcal{R}_{0z} > 1$ .*

**Proof** If we substitute the values of the state variables at the Zika endemic equilibrium into the equation for  $I_{hz}^*$  in (11), we have;

$$\mathcal{H}_1I_{hz}^{*2} + \mathcal{H}_2I_{hz}^* = 0, \tag{15}$$

where  $\mathcal{H}_1 = C_1g_3D_1\mathcal{R}_{0z}^2 + \pi_hg_1D_1$  and  $\mathcal{H}_2 = \mu_zD_1D_2D_3\pi_h(1 - \mathcal{R}_{0z}^2)$ . Since  $\mathcal{H}_1 > 0$ , a unique endemic equilibrium point will exist if  $\mathcal{H}_2 < 0$ , that is, if  $\mathcal{R}_{0z} > 1$ .

### 4 The coinfection model

The coinfection model is a combination of the two sub-models, the malaria sub-model and the Zika sub-model, with the addition of human compartments that are coinfecting with malaria and Zika virus disease. Precisely, the compartments, humans who are coinfecting with both malaria and Zika,  $I_{h mz}$ , and coinfectious humans receiving treatment,  $T_{h mz}$ , are added to the human population. Since there are different mosquitoes that transmit the malaria parasite and Zika virus, there will not be a coinfection case for mosquitoes. Humans that are coinfecting with malaria and Zika virus disease can either transmit malaria to susceptible Anopheles mosquitoes or Zika virus to susceptible Aedes mosquitoes at the probabilities  $\beta_5$  and  $\eta_5$  respectively. Similarly, coinfectious humans that are undergoing treatment for malaria and Zika virus diseases can either transmit malaria to susceptible Anopheles mosquitoes or Zika virus to susceptible Aedes mosquitoes at the probabilities  $\beta_6$  and  $\eta_6$  respectively. The proportion  $\tau_5$  of  $I_{h mz}$  receive treatment for both malaria and Zika virus diseases and recovers at the rate  $\gamma_5$  while the proportions  $\tau_6$  and  $\tau_7$  of  $I_{h mz}$  receive

treatments for only malaria and only zika virus disease respectively. Coinfection of humans occurs when mosquitoes infected with malaria bite humans already infected with the Zika virus and infect them with the malaria parasite or vice versa.

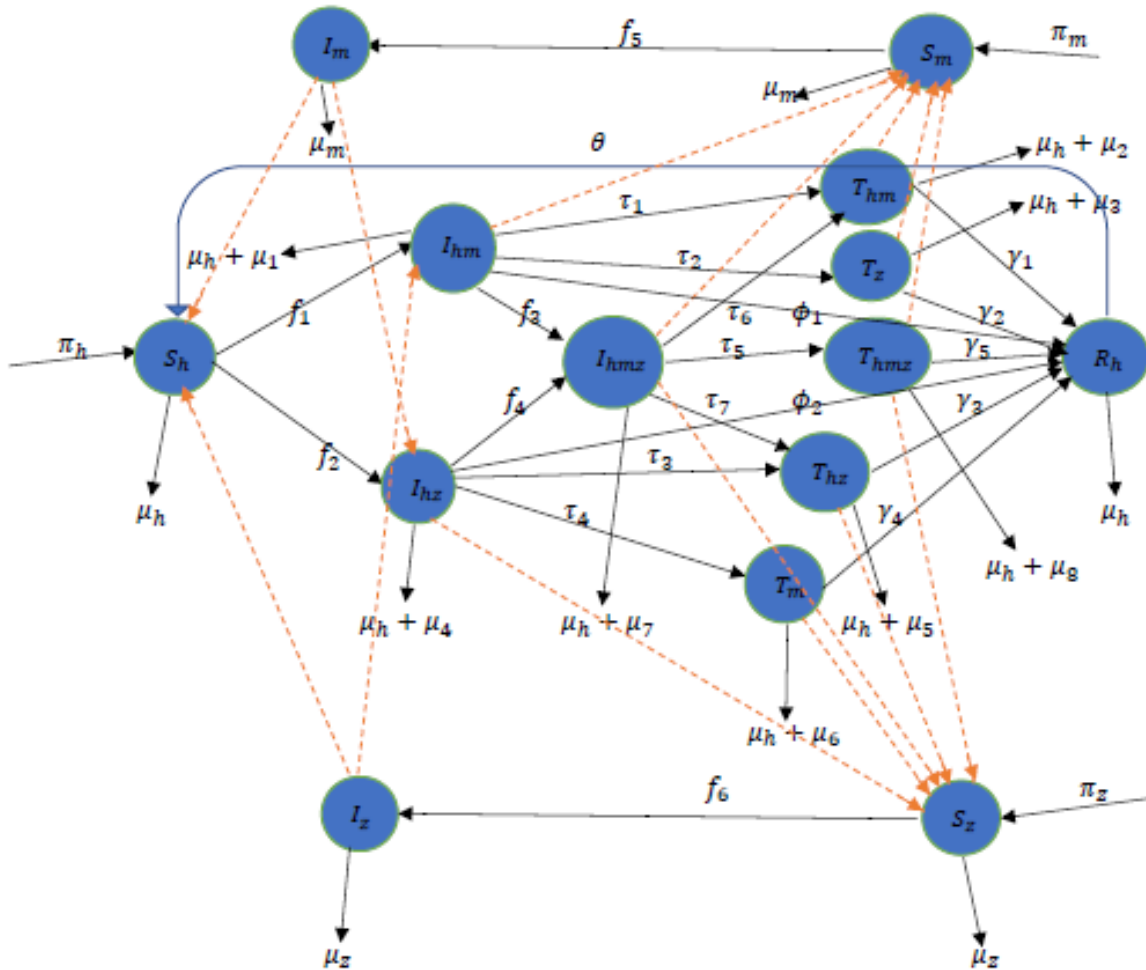


**Figure 3.** Coinfection flow diagram where  $f_1 = \alpha_1\beta_1 I_m(t)$ ,  $f_2 = \alpha_2\eta_1 I_z(t)$ ,  $f_3 = \alpha_2\eta_1 I_z(t)$ ,  $f_4 = \alpha_1\beta_1 I_m(t)$ ,  $f_5 = \alpha_1(\beta_2 I_{hm}(t) + \beta_3 T_{hm}(t) + \beta_4 T_z(t) + \beta_5 I_{hmz}(t) + \beta_6 T_{hmz}(t))$  and  $f_6 = \alpha_2(\eta_2 I_{hz}(t) + \eta_3 T_{hz}(t) + \eta_4 T_m(t) + \eta_5 I_{hmz}(t) + \eta_6 T_{mz}(t))$

The following system of ordinary differential equations describes the coinfection dynamics of the two diseases;

$$\begin{aligned} \frac{dS_h(t)}{dt} &= \pi_h - (\alpha_1\beta_1 I_m(t) + \alpha_2\eta_1 I_z(t))S_h(t) - \mu_h S_h(t) + \theta R_h(t), \\ \frac{dI_{hm}(t)}{dt} &= \alpha_1\beta_1 I_m(t)S_h(t) - \alpha_2\eta_1 I_z(t)I_{hm}(t) - (\tau_1 + \tau_2 + \phi_1 + \mu_h + \mu_1)I_{hm}(t), \\ \frac{dI_{hz}(t)}{dt} &= \alpha_2\eta_1 I_z(t)S_h(t) - \alpha_1\beta_1 I_m(t)I_{hz}(t) - (\tau_3 + \tau_4 + \phi_2 + \mu_h + \mu_4)I_{hz}(t), \\ \frac{dI_{hmz}(t)}{dt} &= \alpha_2\eta_1 I_z(t)I_{hm}(t) + \alpha_1\beta_1 I_m(t)I_{hz}(t) - (\tau_5 + \tau_6 + \tau_7 + \mu_h + \mu_7)I_{hmz}(t), \\ \frac{dT_{hm}(t)}{dt} &= \tau_1 I_{hm}(t) + \tau_6 I_{hmz}(t) - (\gamma_1 + \mu_h + \mu_2)T_{hm}(t), \end{aligned}$$

$$\begin{aligned}
 \frac{dT_z(t)}{dt} &= \tau_2 I_{hm}(t) - (\gamma_2 + \mu_h + \mu_3) T_z(t), \\
 \frac{dT_{hz}(t)}{dt} &= \tau_3 I_{hz}(t) + \tau_7 I_{h mz}(t) - (\gamma_3 + \mu_h + \mu_5) T_{hz}(t), \\
 \frac{dT_m(t)}{dt} &= \tau_4 I_{hz}(t) - (\gamma_4 + \mu_h + \mu_6) T_m(t), \\
 \frac{dT_{h mz}(t)}{dt} &= \tau_5 I_{h mz}(t) - (\gamma_5 + \mu_h + \mu_8) T_{h mz}(t), \\
 \frac{dR_h(t)}{dt} &= \phi_1 I_{hm}(t) + \phi_2 I_{hz}(t) + \gamma_1 T_{hm}(t) + \gamma_2 T_z(t) + \gamma_3 T_{hz}(t) + \gamma_4 T_m + \gamma_5 T_{h mz}(t) - (\mu_h + \theta) R_h(t), \\
 \frac{dS_m(t)}{dt} &= \pi_m - \alpha_1 (\beta_2 I_{hm}(t) + \beta_3 T_{hm}(t) + \beta_4 T_z(t) + \beta_5 I_{h mz}(t) + \beta_6 T_{h mz}(t)) S_m(t) - \mu_m S_m(t), \\
 \frac{dI_m(t)}{dt} &= \alpha_1 (\beta_2 I_{hm}(t) + \beta_3 T_{hm}(t) + \beta_4 T_z(t) + \beta_5 I_{h mz}(t) + \beta_6 T_{h mz}(t)) S_m(t) - \mu_m I_m(t), \\
 \frac{dS_z(t)}{dt} &= \pi_z - \alpha_2 (\eta_2 I_{hz}(t) + \eta_3 T_{hz}(t) + \eta_4 T_m(t) + \eta_5 I_{h mz}(t) + \eta_6 T_{m z}(t)) S_z(t) - \mu_z S_z(t), \\
 \frac{dI_z(t)}{dt} &= \alpha_2 (\eta_2 I_{hz}(t) + \eta_3 T_{hz}(t) + \eta_4 T_m(t) + \eta_5 I_{h mz}(t) + \eta_6 T_{m z}(t)) S_z(t) - \mu_z I_z(t),
 \end{aligned} \tag{16}$$

with initial conditions of the system,  $Z_0 = (S_h^0, I_{hm}^0, I_{hz}^0, I_{h mz}^0, T_{hm}^0, T_z^0, T_{hz}^0, T_m^0, T_{h mz}^0, R_h^0, S_m^0, I_m^0, S_z^0, I_z^0)$ .

### Positivity of solutions and Invariant region for the coinfection model

**Lemma 4** *Given that the initial conditions  $(S_h^0, I_{hm}^0, I_{hz}^0, I_{h mz}^0, T_{hm}^0, T_z^0, T_{hz}^0, T_m^0, T_{h mz}^0, R_h^0, S_m^0, S_z^0, I_m^0, I_z^0) > 0$  to the system, (16) at  $t = 0$  lies in the region,  $\Omega$ , then the solution set  $(S_h(t), I_{hm}(t), I_{hz}(t), I_{h mz}(t), T_{hm}(t), T_z(t), T_{h mz}(t), T_{hz}(t), T_m(t), R_h(t), S_m(t), I_m(t), S_z(t), I_z(t))$  to the system remains positive  $\forall t > 0$ .*

**Proof** From (16), we will have that

$$\frac{dS_h(t)}{dt} \geq -(\alpha_1 \beta_1 I_m(t) + \alpha_2 \eta_1 I_z(t) + \mu_h) S_h(t), \quad \text{and} \quad \frac{dI_z(t)}{dt} \geq -\mu_z I_z(t),$$

which we solve to get

$$S_h(t) \geq S_h^0 e^{-\int_0^t (\alpha_1 \beta_1 I_m(t) + \alpha_2 \eta_1 I_z(t) + \mu_h) dt} > 0, \quad \text{and} \quad I_z(t) \geq I_z^0 e^{-\mu_z t} > 0,$$

respectively. Therefore, the solutions  $S_h(t)$  and  $I_z(t)$  will remain positive for all  $t$  with the given positive initial conditions. Similar results can be obtained for the other variables. This shows that the solution to the coinfection system will remain positive  $\forall t$  provided the initial condition is positive.

Then, from (16), we have that the total human population,  $N_h(t)$ , total Anopheles population  $N_m(t)$  and total Aedes population  $N_z(t)$  satisfy the following differential equations

$$\begin{aligned}
 \frac{dN_h(t)}{dt} &= \pi_h - \mu_h N_h(t) - N_1^*(t), \\
 \frac{dN_m(t)}{dt} &= \pi_m - \mu_m N_m(t), \\
 \frac{dN_z(t)}{dt} &= \pi_z - \mu_z N_z(t),
 \end{aligned} \tag{17}$$



respectively, where  $A_5 = \frac{\alpha_1 \beta_5 \tau_m}{\mu_m}$ ,  $A_6 = \frac{\alpha_1 \beta_6 \tau_m}{\mu_m}$ ,  $B_5 = \tau_5 + \tau_6 + \tau_7 + \mu_h + \mu_7$ ,  $C_5 = \frac{\alpha_2 \eta_5 \tau_z}{\mu_z}$ ,  $C_6 = \frac{\alpha_2 \eta_6 \tau_z}{\mu_z}$  and  $D_5 = \gamma_5 + \mu_h + \mu_8$ . The other  $A_i^s, B_i^s, C_i^s$  and  $D_i^s$  are as described in Section 2 and Section 3 respectively. The non-zero eigenvalues of  $F_{mz} V_{mz}^{-1}$  are  $\{\pm \mathcal{R}_{0m}, \pm \mathcal{R}_{0z}\}$ . Hence, the reproduction number of the coinfection is

$$\mathcal{R}_{mz} = \max(\mathcal{R}_{0m}, \mathcal{R}_{0z}),$$

where  $\mathcal{R}_{0m}$  and  $\mathcal{R}_{0z}$  are as defined in Section 2 and Section 3, respectively.

### Local stability analysis of the coinfection-free equilibrium point

**Theorem 6** *The coinfection-free equilibrium point of the model (16) is locally asymptotically stable if  $\mathcal{R}_{mz} < 1$ , and unstable if  $\mathcal{R}_{mz} > 1$ .*

**Proof** The Jacobian matrix of the coinfection model, evaluated at the coinfection-free equilibrium point  $E_{mz}^0$  has some of its eigenvalues as  $-\mu_h, -(\mu_h + \theta), -\mu_z$ , and  $-\mu_z$ . These eigenvalues are from the non-disease compartments, and the other eigenvalues of the Jacobian matrix are obtained from the submatrix

$$J_1(E_{mz}^0) = \begin{pmatrix} -B_1 & 0 & 0 & 0 & 0 & 0 & 0 & 0 & A_1 & 0 \\ 0 & -D_1 & 0 & 0 & 0 & 0 & 0 & 0 & 0 & C_1 \\ 0 & 0 & -B_5 & 0 & 0 & 0 & 0 & 0 & 0 & 0 \\ \tau_1 & 0 & \tau_6 & -B_2 & 0 & 0 & 0 & 0 & 0 & 0 \\ \tau_2 & 0 & 0 & 0 & -B_3 & 0 & 0 & 0 & 0 & 0 \\ 0 & \tau_3 & \tau_7 & 0 & 0 & -D_2 & 0 & 0 & 0 & 0 \\ 0 & \tau_4 & 0 & 0 & 0 & 0 & -D_3 & 0 & 0 & 0 \\ 0 & 0 & \tau_5 & 0 & 0 & 0 & 0 & -D_5 & 0 & 0 \\ A_2 & 0 & A_5 & A_3 & A_4 & 0 & 0 & A_6 & -\mu_z & 0 \\ 0 & C_2 & C_5 & 0 & 0 & C_3 & C_4 & C_6 & 0 & -\mu_z \end{pmatrix},$$

where  $A_i^s, B_i^s, C_i^s$  and  $D_i^s$  are as described in Section 2, Section 3 and Section 4 respectively. The matrix  $J_1(E_{mz}^0) = F_{mz} - V_{mz}$ . According to [44], all the eigenvalues of  $J_1(E_{mz}^0)$  will have negative real parts if  $\rho(F_{mz} V_{mz}^{-1}) < 1$ . Hence,  $E_{mz}^0$  is locally asymptotically stable if  $\mathcal{R}_{mz} < 1$ , and unstable if  $\mathcal{R}_{mz} > 1$ . The implication of this result is that a small number of malaria and Zika virus-infected humans introduced into the human population will not lead to an outbreak if the reproduction number is less than one, depending on the initial sizes of the infected individuals.

### Global stability analysis of coinfection-free equilibrium point

Lemma 3 was employed in investigating the global stability of the coinfection-free equilibrium point (CFE).

Consider the system of differential equations

$$\frac{dX}{dt} = F(X, 0), \tag{18}$$

$$\frac{dY}{dt} = G(X, Y), G(X, 0) = 0, \tag{19}$$

where  $X = (S_h, R_h, S_m, S_z)$  and  $Y = (I_{hm}, I_{hz}, I_{h mz}, T_{hm}, T_z, T_{hz}, T_m, T_{h mz}, I_m, I_z)$  are the non-disease and disease classes respectively,

$$F = \begin{pmatrix} \pi_h - (\alpha_1\beta_1 I_m + \alpha_2\eta_1 I_z)S_h - \mu_h S_h + \theta R_h \\ \gamma_1 T_{hm} + \gamma_2 T_z + \gamma_3 T_{hz} + \gamma_4 T_m + \gamma_5 T_{h mz} - (\mu_h + \theta)R_h \\ \pi_m - \alpha_1(\beta_2 I_{hm} + \beta_3 T_{hm} + \beta_4 T_z + \beta_5 I_{h mz} + \beta_6 T_{h mz})S_m - \mu_m S_m \\ \pi_z - \alpha_2(\eta_2 I_{hz} + \eta_3 T_{hz} + \eta_4 T_m + \eta_5 I_{h mz} + \eta_6 T_{mz})S_z - \mu_z S_z \end{pmatrix},$$

and

$$G = \begin{pmatrix} \alpha_1\beta_1 I_m S_h - \alpha_2\eta_1 I_z I_{hm} - (\tau_1 + \tau_2 + \mu_h + \mu_1)I_{hm} \\ \alpha_2\eta_1 I_z S_h - \alpha_1\beta_1 I_m I_{hz} - (\tau_3 + \tau_4 + \mu_h + \mu_4)I_{hz} \\ \alpha_2\eta_1 I_z I_{hm} + \alpha_1\beta_1 I_m I_{hz} - (\tau_5 + \tau_6 + \tau_7 + \mu_h + \mu_7)I_{h mz} \\ \tau_1 I_{hm} + \tau_6 I_{h mz} - (\gamma_1 + \mu_h + \mu_2)T_{hm} \\ \tau_2 I_{hm} - (\gamma_2 + \mu_h + \mu_3)T_z \\ \tau_3 I_{hz} + \tau_7 I_{h mz} - (\gamma_3 + \mu_h + \mu_5)T_{hz} \\ \tau_4 I_{hz} - (\gamma_4 + \mu_h + \mu_6)T_m \\ \tau_5 I_{h mz} - (\gamma_5 + \mu_h + \mu_8)T_{h mz} \\ \alpha_1(\beta_2 I_{hm} + \beta_3 T_{hm} + \beta_4 T_z + \beta_5 I_{h mz} + \beta_6 T_{h mz})S_m - \mu_m I_m \\ \alpha_2(\eta_2 I_{hz} + \eta_3 T_{hz} + \eta_4 T_m + \eta_5 I_{h mz} + \eta_6 T_{mz})S_z - \mu_z I_z \end{pmatrix}.$$

Solving  $F$  for  $(S_h, R_h, S_m, S_z)$  as  $t \rightarrow \infty$  to get  $S_h(t) \rightarrow \frac{\pi_h}{\mu_h}, R_h(t) \rightarrow 0, S_m(t) \rightarrow \frac{\pi_m}{\mu_m}, S_z(t) \rightarrow \frac{\pi_z}{\mu_z}$  which corresponds to the values of this state variables at CFE already proven to be locally asymptotically stable. Thus, Eq. (18) is shown to be globally asymptotically stable.

In the system (19), it is required that  $\hat{G}(X, Y) = BY - G(X, Y) \geq 0$ , where  $B$  is the Jacobian matrix of  $G(X, Y)$  evaluated at the coinfection-free equilibrium of the model.

Therefore,

$$\hat{G}(X, Y) = \begin{pmatrix} \alpha_1\beta_1 \left(\frac{\pi_h}{\mu_h} - S_h\right) I_m + \alpha_2\eta_1 I_z I_{hm} \\ \alpha_2\eta_1 \left(\frac{\pi_h}{\mu_h} - S_h\right) I_z + \alpha_1\beta_1 I_m I_{hz} \\ -\alpha_2\eta_1 I_z I_{hm} - \alpha_1\beta_1 I_m I_{hz} \\ 0 \\ 0 \\ 0 \\ 0 \\ 0 \\ \alpha_1 \left(\frac{\pi_m}{\mu_m} - S_m\right) (\beta_2 I_{hm} + \beta_3 T_{hm} + \beta_4 T_z + \beta_5 I_{h mz} + \beta_6 T_{h mz}) \\ \alpha_2 \left(\frac{\pi_z}{\mu_z} - S_z\right) (\eta_2 I_{hz} + \eta_3 T_{hz} + \eta_4 T_m + \eta_5 I_{h mz} + \eta_6 T_{mz}) \end{pmatrix}.$$

From  $\hat{G}(X, Y)$ , we see that  $S_h(t) \leq \frac{\pi_h}{\mu_h}, S_m(t) \leq \frac{\pi_m}{\mu_m}$  and  $S_z(t) \leq \frac{\pi_z}{\mu_z}$ . Thus, only the 3<sup>rd</sup> row is non-negative, and this shows that  $E_{mz}^0$  may not be globally asymptotically stable. Hence, the occurrence of backward bifurcation in the model is a possibility, and the model may not have a unique endemic equilibrium. The possibility of backward bifurcation appearing may be because infectious humans with malaria are re-infected with the Zika virus and vice versa.

### Sensitivity analysis of the model

The sensitivity indices of the parameters in the coinfection reproduction number are shown in Table 2. This analysis helps us to know which parameters have the highest impact on the reproduction number so that they can be targeted as the most effective intervention measure for each case study. By definition, given any dynamical system of infectious disease, the normalized

forward sensitivity index according to [33] of  $\mathcal{R}$  that depends on the parameter  $p$  is given by

$$S_p^{\mathcal{R}} = \frac{\partial \mathcal{R}}{\partial p} \times \frac{p}{\mathcal{R}}, \tag{20}$$

where  $\mathcal{R}$  is the associated reproduction number of the system in discussion and  $p$  is any system parameter in  $\mathcal{R}$ . For our system, the coinfection reproduction number is given by  $\mathcal{R}_{mz} = \max(\mathcal{R}_{0m}, \mathcal{R}_{0z})$ , hence, the sensitivity analysis will be performed on both  $\mathcal{R}_{0m}$  and  $\mathcal{R}_{0z}$ , respectively. The parameters with a positive sensitivity index increase the endemicity of the coinfection, while the parameters with a negative sensitivity index decrease the endemicity of the coinfection.

**Table 2.** Sensitivity index of  $\mathcal{R}_{0m}$  and  $\mathcal{R}_{0z}$

Parameter	Values	Sensitivity index	Parameter	Values	Sensitivity index
$\pi_h$	30	0.5	$\pi_h$	100	0.5
$\pi_m$	30	0.5	$\pi_z$	100	0.5
$\alpha_1$	0.2	1	$\alpha_2$	0.1	1
$\beta_1$	0.034	0.5	$\eta_1$	0.009	0.5
$\beta_2$	0.013	0.2201	$\eta_2$	0.07	0.1210
$\beta_3$	0.0022	0.0923	$\eta_3$	0.03	0.1976
$\beta_4$	0.0044	0.1876	$\eta_4$	0.05	0.1814
$\tau_1$	0.62	-0.2339	$\tau_3$	0.45	-0.0410
$\tau_2$	0.28	0.0403	$\tau_4$	0.35	0.0290
$\mu_h$	0.0556	-0.5001	$\mu_h$	0.0000391	-0.5001
$\mu_m$	0.0556	-1	$\mu_z$	0.0556	-1
$\mu_1$	0.0003454	-0.000182	$\mu_4$	0.0001727	-0.000021
$\mu_2$	0.0001151	-0.000042	$\mu_5$	0.00004	-0.000017
$\mu_3$	0.00001	-0.0003	$\mu_6$	0.00002	-0.000022
$\gamma_1$	0.142	-0.0923	$\gamma_3$	0.1667	-0.1976
$\gamma_2$	0.111	-0.1872	$\gamma_4$	0.118	-0.1813
$\phi_1$	0.05	-0.0263	$\phi_2$	0.1429	-0.0758

Hence, to control the coinfection, the parameters with negative values need to be increased while those with positive values need to be reduced. This means that those parameters with positive values needs much attention as controlling them will significantly reduce the spread of the disease. The parameter with the highest impact on the spread of the disease is the contact rate of humans with the mosquitoes, denoted by  $\alpha_1$  and  $\alpha_2$ , with sensitivity indices of 1 respectively. Thus, successful control of the coinfection or the individual infections will require ensuring that the mosquitoes have minimal contact with humans. This will also reduce the probabilities of transmission of malaria and Zika virus disease from humans to mosquitoes and vice versa, represented by the parameters,  $\beta_i$ 's and  $\eta_i$ 's whose sensitivity indices are all positive. We could also see that wrong diagnoses and wrong treatment, represented by  $\tau_2$  and  $\tau_4$  respectively, also increase the individual infections as well as the coinfection of humans. The sensitivity results also showed that an increase in the rate of recruiting humans or mosquitoes will definitely make the diseases persist, as more human and vector carriers are made available. The parameters with negative values do not increase the persistence of the coinfection. The parameter with the least negative value is  $\mu_m$  and  $\mu_z$ , which represent the natural death rate of mosquitoes. This means that to control the disease, efforts should also be focused on ensuring that the mosquitoes die more often, as this will also reduce the population of the mosquitoes and hence the contact rate of the mosquitoes with humans. The sensitive indices for  $\pi_h$ ,  $\pi_m$  and  $\pi_z$  which represents recruitment rates for humans,

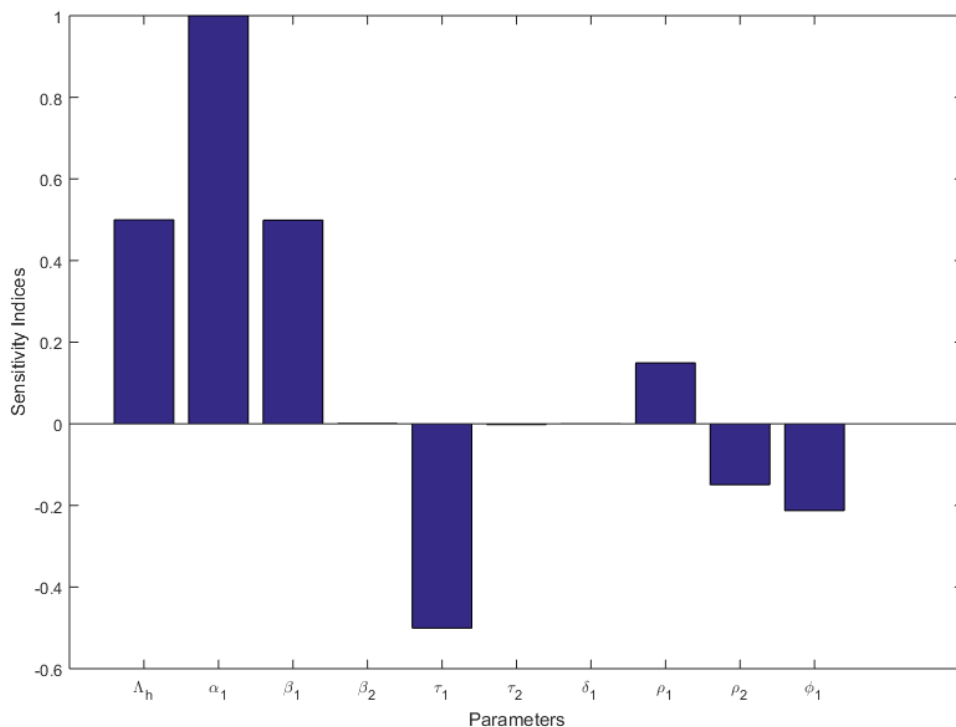


**Figure 4.** Sensitivity plots of parameters of  $R_{0m}$

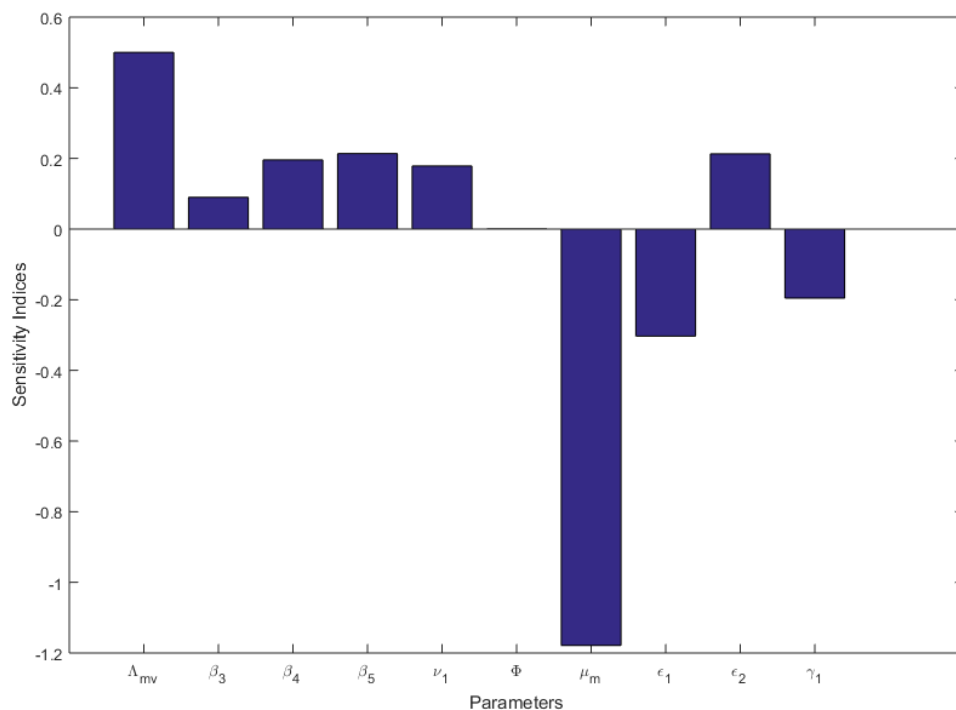


**Figure 5.** Sensitivity plots of parameters of  $R_{0m}$  cont'd

anopheles and aedes mosquitoes respectively showed that one strategy to curb the coinfection is for humans to avoid areas where these mosquitoes are prevalent and efforts should be made to

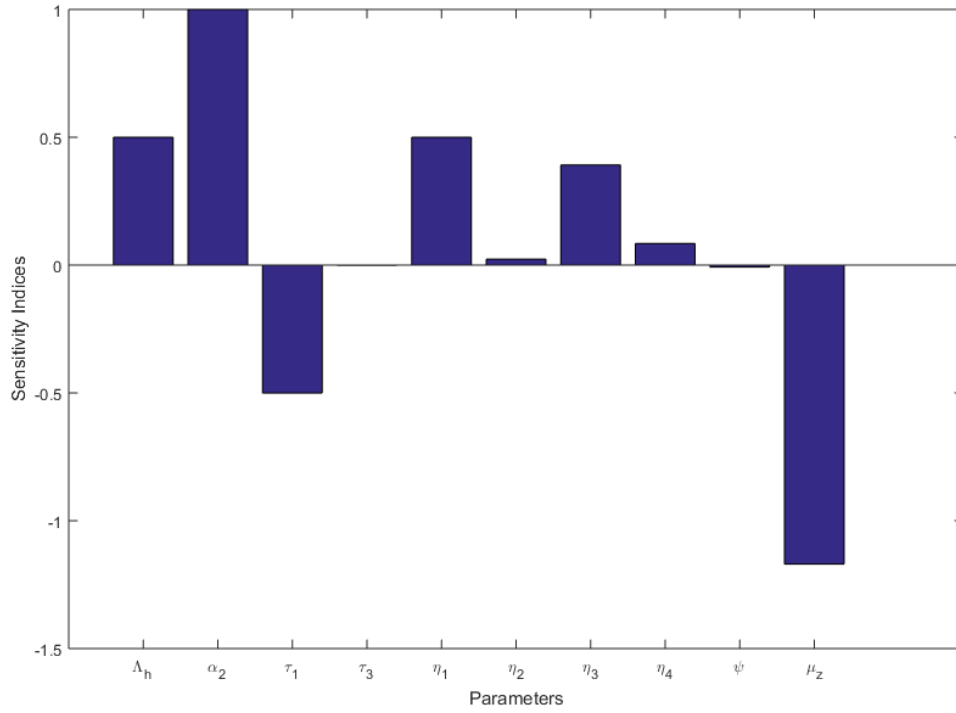


Figure 6. Sensitivity plots of parameters of  $R_{0z}$

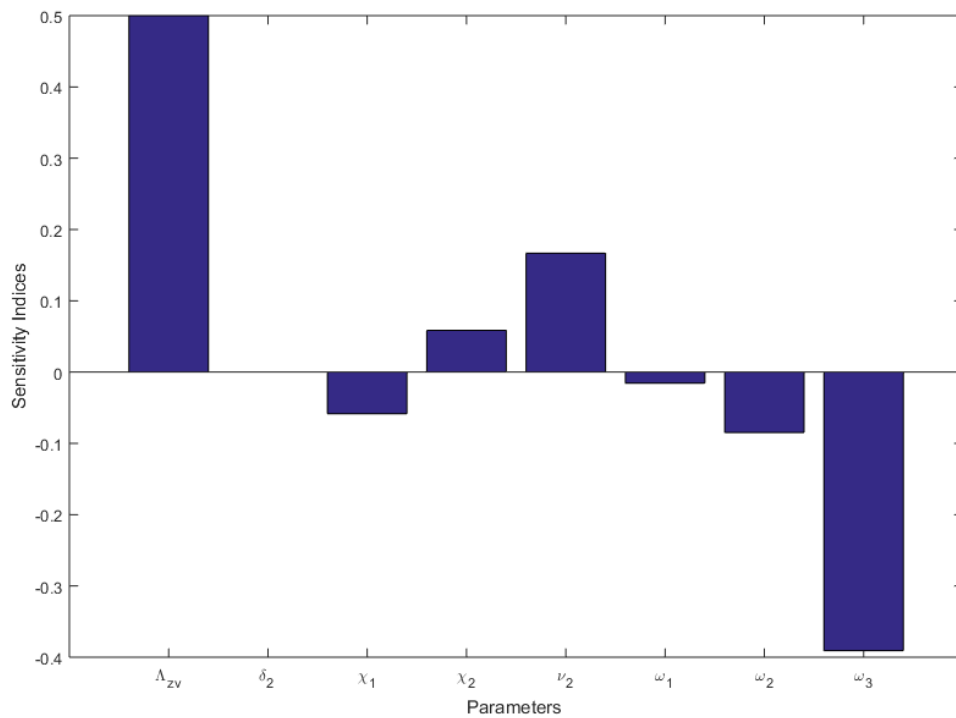


Figure 7. Sensitivity plots of parameters of  $R_{0z}$  cont'd

reduce the recruitment of more mosquitoes into human environment.

## 5 Numerical simulations

Numerical simulations are carried out in this section to graphically illustrate some of the results obtained in this work. The simulations were done using the assumed initial data;  $S_h = 500$ ,  $I_{hm} = 32$ ,  $I_{hz} = 29$ ,  $I_{hmz} = 24$ ,  $T_{hm} = 13$ ,  $T_z = 17$ ,  $T_{hmz} = 12$ ,  $T_{hz} = 15$ ,  $T_m = 12$ ,  $R_h = 20$ ,  $S_m = 500$ ,  $I_m = 90$ ,  $S_z = 500$ , and  $I_z = 50$  and parameter values in [Table 3](#). The results of the numerical experiments are shown in [Figure 8-Figure 14](#) below. The simulations were carried out using MATLAB<sup>®</sup> R2014b, where the fourth-order Runge-Kutta integration scheme is used to obtain a numerical solution to the non-linear system. Some of the parameter values were obtained from the literature, while others were assumed to be within a reasonable and realistic range for the purpose of the simulation.

**Table 3.** Parameter values used in this model

Parameter	Value	Source	Parameter	Value	Source
$\pi_h$	100	assumed	$\alpha_1$	0.2	assumed
$\pi_m$	100	[42]	$\alpha_2$	0.1	[33]
$\pi_z$	100	[39]	$\tau_1$	0.62	[33]
$\mu_1$	0.0003454	[6, 42]	$\tau_2$	0.28	assumed
$\mu_2$	0.0001151	assumed	$\tau_3$	0.45	assumed
$\mu_h$	0.0000391	[9, 41]	$\tau_4$	0.35	assumed
$\mu_3$	0.0001727	assumed	$\tau_5$	0.35	assumed
$\mu_4$	0.00004	assumed	$\tau_6$	0.32	assumed
$\mu_5$	0.00001	assumed	$\tau_7$	0.28	assumed
$\mu_6$	0.00002	assumed	$\theta$	0.143	[5]
$\mu_7$	0.0003454	assumed	$\mu_8$	0.0001927	assumed
$\mu_m$	0.0556	[9]	$\gamma_1$	0.25	[5]
$\mu_z$	0.0556	[9]	$\gamma_2$	0.111	assumed
$\gamma_3$	0.118	[33]	$\gamma_4$	0.1667	[9]
$\beta_1$	0.0022	[28]	$\eta_1$	0.09	[33, 35]
$\beta_2$	0.013	[6]	$\eta_2$	0.07	[9]
$\beta_3$	0.0022	[41]	$\eta_3$	0.03	[33]
$\beta_4$	0.0044	[41]	$\eta_4$	0.05	assumed
$\beta_5$	0.0022	assumed	$\eta_5$	0.03	assumed
$\beta_6$	0.0044	assumed	$\eta_6$	0.02	assumed
$\gamma_5$	0.111	[33]	$\phi_1$	0.05	assumed
$\phi_2$	0.1429	[26]			

### Sub-models

The simulation of the malaria and Zika sub-models is shown in [Figure 8](#) and [Figure 9](#) below. In [Figure 8](#), it is shown that an increase in wrong treatment increases the total infectious human population with malaria, while an increase in right treatment reduces the total infectious human population with malaria. [Figure 9a](#) shows how increasing the rate of right treatment reduces the infectious human population with Zika, while [Figure 9b](#) shows the impact of wrong treatment on the infectious human population. An increase in the rate of wrong treatment leads to an increase in the infectious human population, thereby making it difficult to control the disease. This result shows that effective treatment is significant in controlling infectious diseases and must be encouraged by health practitioners. Hence, proper diagnosis of the disease is crucial to controlling it, and efforts should be made by health practitioners to discourage self-diagnosis and self-treatment.

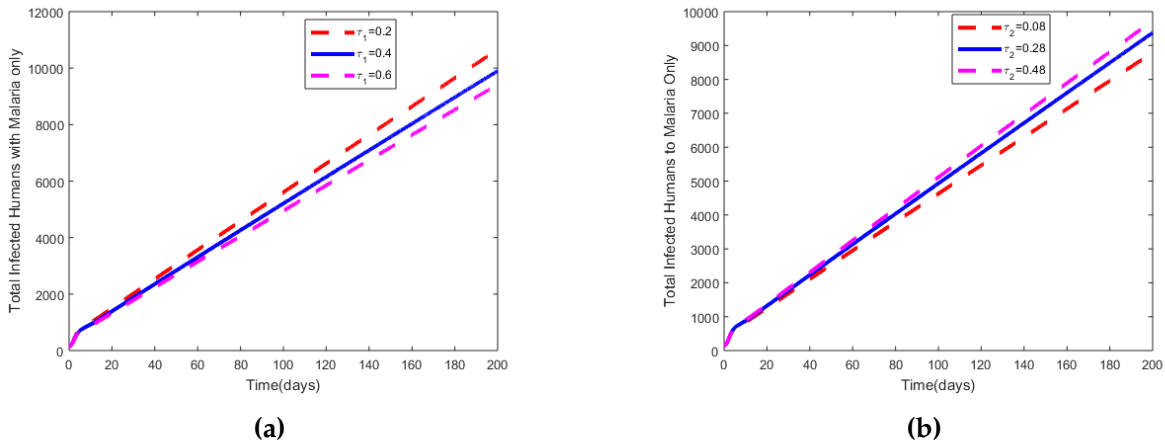


Figure 8. Effect of increase in rate of (a) right treatment,  $\tau_1$  and (b) wrong treatment,  $\tau_2$

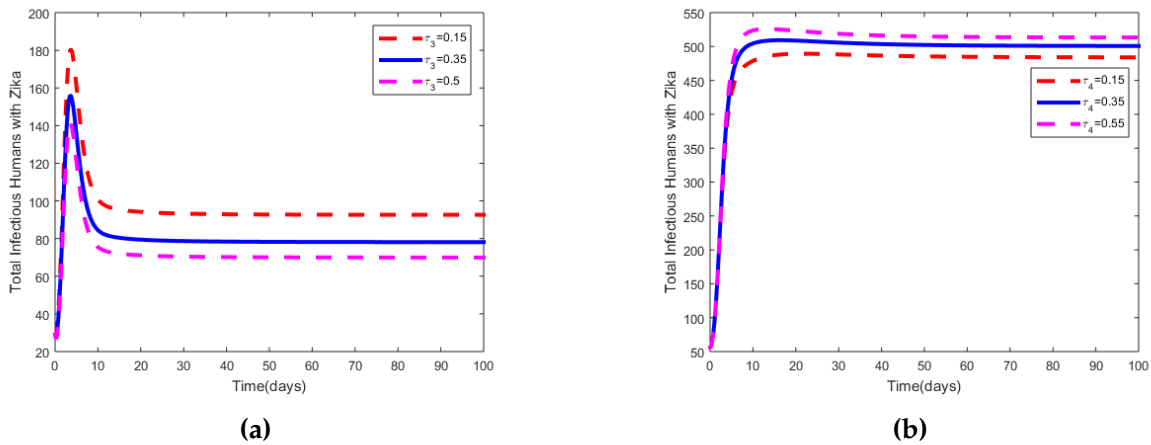


Figure 9. Effect of increase in right treatment,  $\tau_3$  and wrong treatment,  $\tau_4$

### Coinfection model

The effect of misdiagnoses and wrong treatment in the coinfecting human population is shown in Figure 10 and Figure 11, where we see that as the rate at which infectious humans with malaria or Zika undergoing right treatment,  $\tau_1$  or  $\tau_3$  increases, the total infected humans also decreases. This shows that the right treatment reduces the population of the total infectious classes. Similarly, as the rate at which infectious humans with malaria or Zika, that undergo the wrong treatment  $\tau_2$  or  $\tau_4$ , increases, the total infected humans also increases. This implies that wrong diagnoses and wrong treatment play a significant role in the dynamics of the diseases and hence should be avoided. Figure 12 shows the impact of the increase in the population of Anopheles mosquitoes on Aedes mosquitoes and vice versa.

Particularly, it shows that in any environment where Anopheles and Aedes mosquitoes coexist, an increase in the population of one will lead to an increase in the other. This proportionality relationship is in line with real-life situations, as both mosquito populations are affected by the same environmental factors.

In Figure 13, we see that an increase in the contact rate of humans with Anopheles mosquitoes increases the total infectious classes of both humans and mosquitoes with malaria. This is because the more mosquitoes come in contact with humans during a blood meal, the more the chances of humans infecting mosquitoes or mosquitoes infecting humans. This result corroborates existing

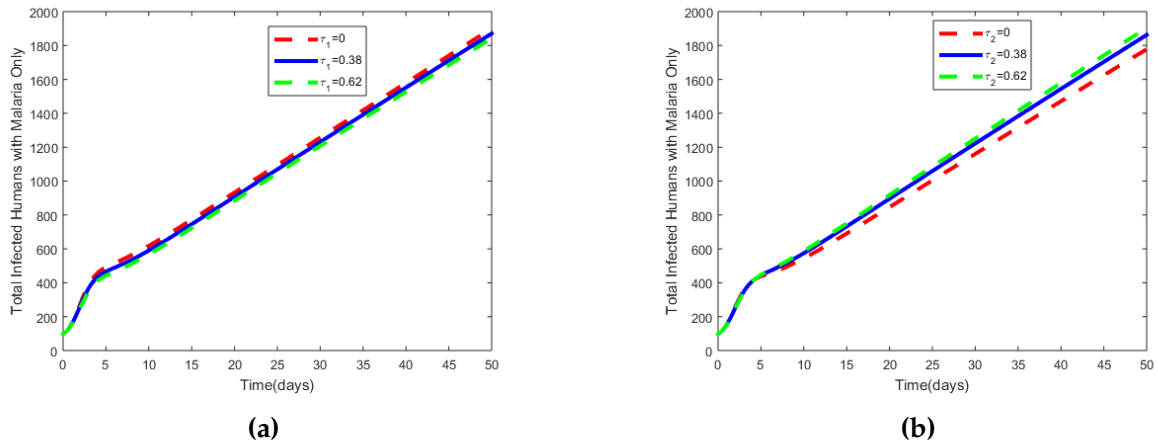


**Figure 10.** Malaria-infected humans for increasing  $\tau_1$  and  $\tau_2$

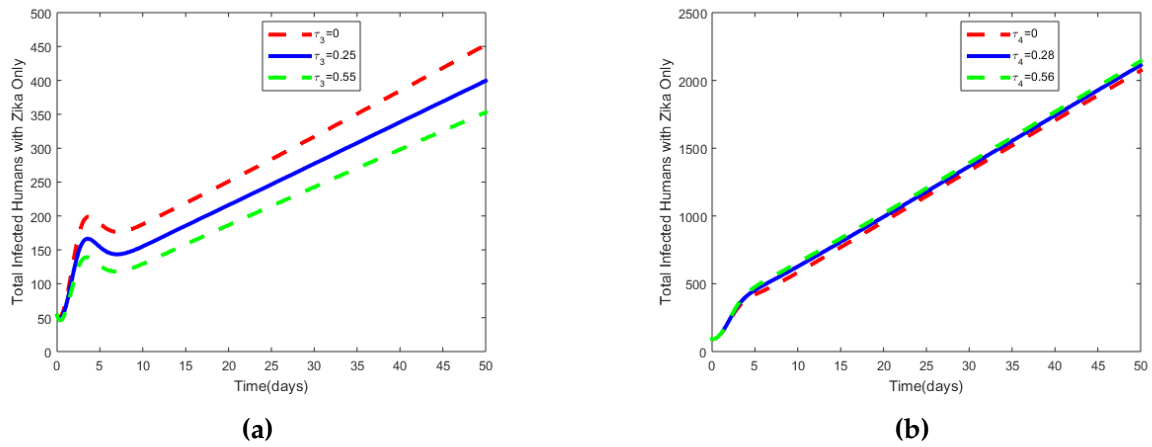


**Figure 11.** Zika-infected humans for increasing  $\tau_3$  and  $\tau_4$

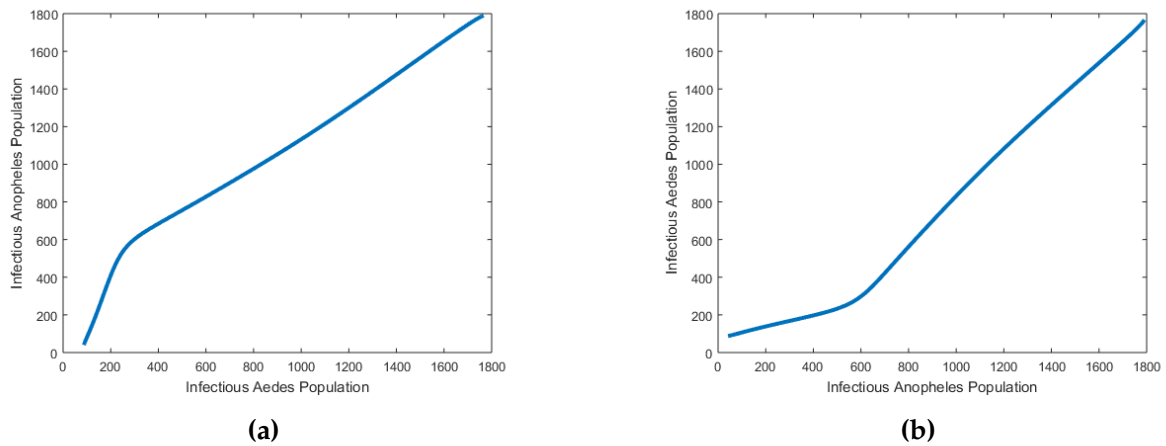


**Figure 12.** (a) Graph of  $I_m$  vs  $I_z$  and (b) Graph of  $I_z$  vs  $I_m$

knowledge that one of the effective ways of controlling malaria is to adopt strategies that reduce human contact with the vector.

In [Figure 14](#), it is also shown that as the rate of contact between humans and Aedes mosquitoes increases, the infectious class with Zika virus disease in both humans and mosquitoes also

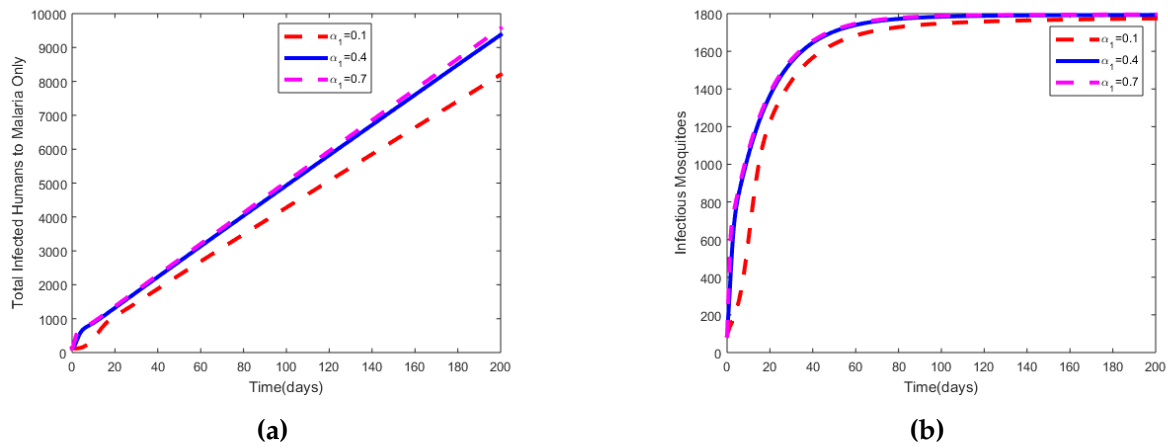


Figure 13. Effect of increase in human contact rate with Anopheles mosquitoes

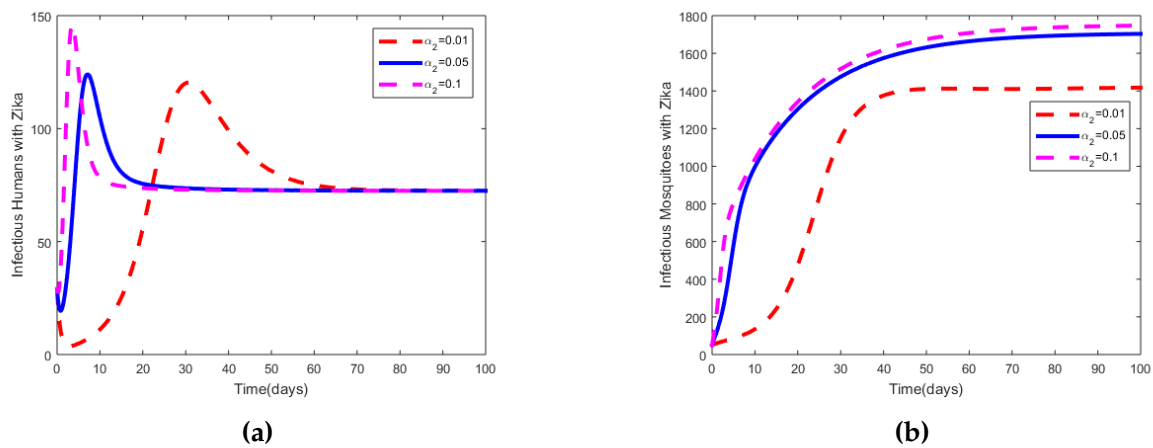


Figure 14. Effect of increase in human contact rate with Aedes mosquitoes

increases. This increase is because the more humans come in contact with mosquitoes, the higher the probability of infection. This shows that one of the ways of controlling the spread of the disease is to ensure the rate of contact of humans with mosquitoes is reduced by implementing measures that will reduce the population of mosquitoes.

## 6 Conclusion

In this paper, we presented a new model that describes the dynamics of malaria, Zika virus, and their coinfection in the presence of wrong treatment. The diseases were modeled using systems of nonlinear ordinary differential equations, which describe their dynamics in human and mosquito populations. The disease-free equilibria of the individual models were shown to be both locally and globally asymptotically stable when their basic reproduction numbers were less than one. However, for the coinfection model, the disease-free equilibrium is locally asymptotically stable but may not be globally stable when the  $\mathcal{R}_{mz} < 1$ . This possibility of global instability is a result of the reinfection of malaria-infected humans with the Zika virus and vice versa. This is also an indication that the coinfection model may not possess a unique endemic equilibrium, which is locally asymptotically stable when  $\mathcal{R}_{mz} > 1$ . The result of the effect of misdiagnosis of each of the diseases shows that if the proportion of those who are wrongly diagnosed and wrongly treated increases, the total infected population of humans with that disease also increases. The results also showed that an increase in the rate of right treatment increases the recovery rate of infectious

humans and reduces the population of the infectious class. Plots from the numerical experiments were used to show these results. Sensitivity analysis also showed that mosquito contact rate with humans and the probability of infecting humans during such contacts were the more sensitive parameters in the system, hence efforts in effective controlling of the diseases or their coinfection must incorporate reduction of these parameters. The wrong treatment of each disease as the other is shown to also affect the endemicity of the two diseases. The sensitivity analysis further highlights that if there is less recruitment of mosquitoes or their natural death rates are increased, then the diseases can be controlled.

Conclusively, wrong treatment has been shown to play a major role in the spread of malaria and Zika virus diseases, as well as their coinfection in any environment where the two diseases coexist. Therefore, it is recommended that treating infectious humans with respect to the symptoms they manifest should be avoided. Clinical analysis should always be conducted to avoid a wrong diagnosis. In addition, since the disease-free equilibrium may not be globally asymptotically stable, extra effort should be made in order to eradicate the two diseases. Further research work in this regard will require investigating the effects of other control measures, other than treatment, in the co-circulation and coinfection of the diseases.

### **Declarations**

#### **Use of AI tools**

The authors declare that they have not used Artificial Intelligence (AI) tools in the creation of this article.

#### **Data availability statement**

All data generated or analyzed during this study are included in this article.

#### **Ethical approval**

The authors state that this research complies with ethical standards. This research does not involve either human participants or animals.

#### **Consent for publication**

Not applicable

#### **Conflicts of interest**

The authors declare that they have no conflict of interest.

#### **Funding**

Not applicable

#### **Author's contributions**

E.C.D.: Methodology, Software, Validation, Visualization, Formal Analysis, Writing - Original Draft, M.C.A.: Investigation, Writing - Original Draft, Visualization, Methodology, Validation, Supervision, Project Administration, G.C.E.M.: Writing-Review & Editing, Validation, Supervision, Project Administration. The authors have read and agreed to the published version of the manuscript.

## Acknowledgements

The authors would like to thank the anonymous reviewers for their helpful comments and feedback, which greatly strengthened the overall manuscript.

## References

- [1] McArdle, A.J., Turkova, A. and Cunnington, A.J. When do co-infections matter? *Current Opinion in Infectious Diseases*, 31(3), 209-215, (2018). [[CrossRef](#)]
- [2] World Health Organization, Tuberculosis and HIV, (2023). <https://www.who.int/hiv/topics/tb/en/index.html>
- [3] Boulaaras, S., Yavuz, M., Alrashedi, Y., Bahramand, S. and Jan, R. Modeling the co-dynamics of vector-borne infections with the application of optimal control theory. *Discrete and Continuous Dynamical Systems-S*, 18(5), 1331-1352, (2025). [[CrossRef](#)]
- [4] Bolaji, B., Onoja, T., Benedict, A.C., Omede, B.I. and Odionyenma, U.B. Dynamical analysis of HIV-TB co-infection transmission model in the presence of treatment for TB. *Bulletin of Biomathematics*, 2(1), 21-56, (2024). [[CrossRef](#)]
- [5] Onah, S.I., Collins, O.C., Okoye, C. and Mbah, G.C.E. Dynamics and control measures for malaria using a mathematical epidemiological model. *Electronic Journal of Mathematical Analysis and Applications*, 7(1), 65-73, (2019).
- [6] Nwankwo, A. and Okuonghae, D. Mathematical assessment of the impact of different micro-climate conditions on malaria transmission dynamics. *Mathematical Biosciences and Engineering*, 16(3), 1414-1444, (2019). [[CrossRef](#)]
- [7] World Health Organization, World Malaria Report 2023, (2023). <https://www.who.int/topics/malaria/en/>
- [8] Atokolo, W. and Mbah Christopher Ezike, G. Modeling the control of zika virus vector population using the sterile insect technology. *Journal of Applied Mathematics*, 2020(1), 6350134, (2020). [[CrossRef](#)]
- [9] Lamwong, J. and Pongsumpun, P. Age structural model of Zika virus. *International Journal Modeling and Optimization*, 8(1), 17-23, (2018). [[CrossRef](#)]
- [10] World Health Organization, The History of Zika virus, (2016). <https://www.who.int/news-room/feature-stories/detail/the-history-of-zika-virus>
- [11] Centers for Disease Control and Prevention (CDC), Responds to ZIKA. Zika Virus: Information for Clinicians, (2022). <https://www.cdc.gov/zika/pdfs/clinicianppt>
- [12] Osman, M.A.E., Yang, C. and Adu, I.K. Mathematical model of malaria transmission with optimal control in democratic republic of the Congo. *Global Journal of Science Frontier Research: F Mathematics and Decision Sciences*, 19(1), 1-23, (2019).
- [13] Oke, S., Adeniyi, M.O., Ojo, M.M. and Matadi, M.B. Mathematical modeling of malaria disease with control strategy. *Communication in Mathematical Biology and Neuroscience*, 43, 1-29, (2020). [[CrossRef](#)]
- [14] Omale, D., Omale, J.P. and Atokolo, W. Mathematical Modeling on the Transmission Dynamics and Control of Malaria with Treatment within a Population. *Academic Journal of Statistics and Mathematics*, 6(2), 15-30, (2020).
- [15] Fatmawati, F., Herdicho, F.F., Windarto, Chukwu, W. and Tasman, H. An optimal control of malaria transmission model with mosquito seasonal factor. *Results in Physics*, 25, 104238, (2021). [[CrossRef](#)]

- [16] Aldila, D. Dynamical analysis on a malaria model with relapse preventive treatment and saturated fumigation. *Computational Mathematics and Methods in Medicine*, 2022(1), 135452, (2022). [[CrossRef](#)]
- [17] Keno, T.D., Dano, L.B. and Makinde, O.M. Modeling and optimal control analysis for malaria transmission with role of climate variability. *Computational Mathematics Methods*, 2022(1), 9667396, (2022). [[CrossRef](#)]
- [18] Collins, O.C. and Duffy, K.J. A mathematical model for the dynamics and control of malaria in Nigeria. *Infectious Disease Modelling*, 7(4), 728-741, (2022). [[CrossRef](#)]
- [19] Al Basir, F. and Abraha, T. Mathematical modelling and optimal control of malaria using awareness-based interventions. *Mathematics*, 11(7), 1687, (2023). [[CrossRef](#)]
- [20] Alhaj, M.S. Mathematical model for malaria disease transmission. *Journal of Mathematical Analysis and Modelling*, 4(1), 1-16, (2023). [[CrossRef](#)]
- [21] Witbooi, P.J., Vyambwera, S.M., Van Schalkwyk, G.J. and Muller, G.E. Stability and control in a stochastic model of malaria population dynamics. *Advances in Continuous and Discrete Models*, 2023, 43, (2023). [[CrossRef](#)]
- [22] Eguda, F.Y., Andrawus, J., Stephen, I.M. and Sale, A. Modeling the spread of Zika virus with vaccination and vector reduction as control strategies. *Dutse Journal Pure and Applied Sciences*, 5, 273–284, (2019).
- [23] Rakkiyappan, R., Latha, V.P. and Rihan, F.A. A fractional-order model for Zika virus infection with multiple delays. *Complexity*, 2019(1), 4178073, (2019). [[CrossRef](#)]
- [24] Biswas, S.K., Ghosh, U. and Sarkar, S. Mathematical model of zika virus dynamics with vector control and sensitivity analysis. *Infectious Disease Modelling*, 5, 23-41, (2019). [[CrossRef](#)]
- [25] Gonzalez-Parra, G. and Benincasa, T. Mathematical modeling and numerical simulations of Zika in Colombia considering mutation. *Journal of Mathematical Computations and Simulations*, 163, 1-18, (2019). [[CrossRef](#)]
- [26] Andayani, P., Sari, L.R., Suryanto, A. and Darti, I. Numerical study for ZIKA virus transmission with Beddington–Deangelis incidence rate. *Far East Journal Mathematical Science*, 111(1), 145-157, (2019). [[CrossRef](#)]
- [27] Anyanwu, M.C., Mbah, G.C.E. and Duru, E.C. On mathematical model for zika virus disease control with wolbachia-infected mosquitoes. *Abacus (Mathematical Science Series)*, 47(1), 35–54, (2020).
- [28] Amoah-Mensah, J., Dontwi, J. and Bonyah, E. Stability analysis of Zika–malaria co-infection model for malaria endemic region. *Journal of Advances in Mathematics and Computer Science*, 26(1), 1-22, (2018). [[CrossRef](#)]
- [29] Hussein, R., Guedes, M., Ibraheim, N., Ali, M.M., El-Tahir, A., Allam, N. et al. Impact of COVID-19 and malaria coinfection on clinical outcomes: a retrospective cohort study. *Clinical Microbiology and Infection*, 28(8), 1152.e1-1152.e6, (2022). [[CrossRef](#)]
- [30] Otu, A.A., Udoh, U.A., Ita, O.I., Hicks, J.P., Ukpeh, I. and Walley, J. Prevalence of Zika and malaria in patients with fever in secondary healthcare facilities in south-eastern Nigeria. *Tropical Doctor*, 50(1), 22–30, (2020). [[CrossRef](#)]
- [31] Mac, P.A., Kroeger, A., Daehne, T., Anyaike, C., Velayudhan, R. and Panning, M. Zika, flavivirus and malaria antibody cocirculation in Nigeria. *Tropical Medicine and Infectious Disease*, 8(3), 171, (2023). [[CrossRef](#)]

- [32] Anyanwu, M.C. and Duru, E.C. Modeling the effect of misdiagnosis in the co-circulation and co-infection of dengue and Zika virus disease. *Journal of Mathematical Analysis and Modelling*, 4(2), 59-79, (2023). [[CrossRef](#)]
- [33] Duru, E.C., Mbah, G.C.E., Anyanwu, M.C. and Nnamani, T.N. Modelling the co-infection of malaria and zika virus disease. *Journal of Nigerian Society for Physical Sciences*, 6(2), 1938, (2024). [[CrossRef](#)]
- [34] Baba, M.M., Ahmed, A., Jackson, S.Y. and Oderinde, B.S. Cryptic Zika virus infections unmasked from suspected malaria cases in Northeastern Nigeria. *PLoS ONE*, 18(11), e0292350, (2023). [[CrossRef](#)]
- [35] Bonyah, E., Khan, M.A., Okosun, K.O. and Gomez-Aguilar, J.F. On the co-infection of dengue fever and Zika virus. *Optimal Control and Applied Mathematics*, 40(3), 394-421, (2018). [[CrossRef](#)]
- [36] Ogunmiloru, O.M. Mathematical modeling of the coinfection dynamics of malaria-toxoplasmosis in the tropics. *Biometrical Letters*, 56(2), 139-163, (2019). [[CrossRef](#)]
- [37] Moya, E.D., Rodrigues, D.S., Pietrus, A. and Severo, A.M. A mathematical model for HIV/AIDS under pre-exposure and post-exposure prophylaxis. *Biomath*, 11(2), 1-28, (2022). [[CrossRef](#)]
- [38] Moya, E.D., Rodriguez, R.A. and Pietrus, A. A mathematical model for the study of HIV/AIDS transmission with PrEP coverage increase and parameter estimation using MCMC with a Bayesian approach. *Bulletin of Biomathematics*, 2(2), 218-244, (2024) [[CrossRef](#)]
- [39] Duru, E.C., Mbah, G.C.E. and Uzoma, A. Numerical simulations and solutions of a mathematical model for Zika virus disease. *Applications of Modelling and Simulations*, 9(1), 139-153, (2025).
- [40] Kiemtore, A., Sawadogo, W.O., Ouédraogo, P.O.F., Aqel, F., Alaa, H., Somda, K.S. and Serme, A.K. Mathematical modelling of the impact of vaccination, treatment and media awareness on the hepatitis B epidemic in Burkina Faso. *Mathematical Modelling and Numerical Simulation with Applications*, 4(5), 139-164, (2024). [[CrossRef](#)]
- [41] Duru, E.C. and Mbah G.C. Approximate solution for a malaria model using the homotopy analysis method. *Biometrical Letters*, 1-27, (2025). [[CrossRef](#)]
- [42] Duru, E.C., Mbah, G.C., Anyanwu, M.C. and Nwosu, C.N. Mathematical modelling of malaria with vaccination, treatment and vector control. *International Journal of Biomathematics*, 18(11), 1-29, (2025). [[CrossRef](#)]
- [43] Mustapha, U.T., Maigoro, Y.A., Yusuf, A. and Qureshi, S. Mathematical modeling for the transmission dynamics of cholera with an optimal control strategy. *Bulletin of Biomathematics*, 2(1), 1-20, (2024). [[CrossRef](#)]
- [44] Van Den Driessche, P. and Watmough, J. Reproduction numbers and sub-threshold endemic equilibria for compartmental models of disease transmission. *Mathematical Biosciences*, 180(1-2), 29-48, (2002). [[CrossRef](#)]
- [45] Omede, B.I., Peter, O.J., Atokolo, W., Bolaji, B. and Ayoola, T.A. A mathematical analysis of the two-strain tuberculosis model dynamics with exogenous re-infection. *Healthcare Analytics*, 4, 100266, (2023). [[CrossRef](#)]
- [46] Mani, D.N.P., Shanmugam, M., Yavuz, M. and Muthuradhinam, S. Dynamic behaviour of an eco-epidemiological model of fractional-order with a fear effect. *Journal of Applied Mathematics and Computing*, 1-25, (2025). [[CrossRef](#)]
- [47] Castillo-Chavez, C. and Song, B. Dynamical models of tuberculosis and their applications.

*Mathematical Biosciences and Engineering*, 1(2), 361-404, (2004). [[CrossRef](#)]

- [48] Saravanan, S. and Monica, C. Dynamics of a stochastic SEIQR model: stationary distribution and disease extinction with quarantine measures. *Mathematical Modelling and Numerical Simulation with Applications*, 5(1), 172-197, (2025). [[CrossRef](#)]

Bulletin of Biomathematics (BBM)  
(<https://dergipark.org.tr/en/pub/bulletinbiomath>)



**Copyright:** © 2025 by the authors. This work is licensed under a Creative Commons Attribution 4.0 (CC BY) International License. The authors retain ownership of the copyright for their article, but they allow anyone to download, reuse, reprint, modify, distribute, and/or copy articles in *BBM*, so long as the original authors and source are credited. To see the complete license contents, please visit (<http://creativecommons.org/licenses/by/4.0/>).

**How to cite this article:** Duru, E.C., Anyanwu, M.C. & Mbah, G.C.E. (2025). A mathematical model to investigate the effect of misdiagnosis and wrong treatment in the co-circulation and co-infection of Malaria and Zika virus disease. *Bulletin of Biomathematics*, 3(1), 79-110. <https://doi.org/10.59292/bulletinbiomath.1711811>